Inhibitor selectivity: profiling and prediction

Janssen, A.P.A.

I may not have gone where I intended to go, but I think I have ended up where I needed to be.
Douglas Adams

5

BIA 10-2474 is a non-selective FAAH inhibitor that disrupts lipid metabolism

Part of this research was published in A.C.M. van Esbroeck, A.P.A. Janssen *et al. Science* **356**, 1084–1087 (2017).

Introduction

In January 2016, a first-in-human study of the fatty acid amide hydrolase (FAAH) inhibitor BIA 10-2474 led to the death of one volunteer and the hospitalization of four others.[1–4] All patients manifested mild-to-severe neurological symptoms.[3] FAAH is a membrane-bound serine hydrolase that degrades the endocannabinoid anandamide and related amidated lipids.[5–8] Three explanations for the clinical neurotoxicity of BIA 10-2474 have been proposed: (i) errors may have occurred in the clinical trial itself, either in the manufacturing or handling of the compound or in the conduct of the trial; (ii) through its inhibitory effects on FAAH, BIA 10-2474 may have produced high levels of long-chain fatty acid amides (e.g.,

anandamide) and their oxygenated metabolites, which could potentially overstimulate cannabinoid CB_1[8], TRPV1[9], and/or NMDA receptors[10]; or (iii) BIA 10-2474 and/or its metabolites might have off-target activities. The first hypothesis was dismissed by the French authorities.[4] The second hypothesis is considered unlikely because other FAAH inhibitors, such as PF-04457845, have exhibited favourable safety profiles in phase 1 and 2 clinical trials.[11,12] No information has previously been made available regarding the protein interaction profile of BIA 10-2474 that could help in defining the cause of its clinical toxicity, and in particular to directly evaluate the third hypothesis – the possibility that the observed clinical neurotoxicity might have resulted from off-target activity.[1] Therefore, aided by chemical proteomic methods for mapping the interaction landscapes of (ir)reversible serine hydrolase inhibitors[13–17], the serine hydrolase target selectivity of BIA 10-2474 versus other widely used FAAH inhibitors was desired. To this end a comparative study was set up to determine and compare the interaction profiles of BIA 10-2474, its major metabolite BIA 10-2639, the clinically safe PF-04457845 and URB597.

Results

BIA 10-2474 (Figure 5.1A) contains an electrophilic imidazole urea that may react with the nucleophilic serine of FAAH and other serine hydrolases to form covalent and irreversible adducts. On the basis of previously developed chemical proteomic methods to map the interaction landscapes of (ir)reversible serine hydrolase inhibitors,[13–17] it was anticipated that the serine hydrolase targets of BIA 10-2474 could be identified and compared to the selectivity profiles of other widely used FAAH inhibitors, such as URB597[6] and the clinical candidate PF-04457845.[18] PF-04457845 progressed to phase 2 trials without serious adverse events.[18] Therefore, BIA 10-2474 along with BIA 10-2639, a confirmed metabolite in which the *N*-oxide is reduced to a pyridine, were synthesized.[4] These compounds were tested for inhibition of FAAH-catalysed conversion of [^{14}C]-anandamide to arachidonic acid and [^{14}C]-ethanolamine.[19] Surprisingly, BIA 10-2474 showed very weak inhibitory activity (IC_{50} > 1 µM) against the FAAH species tested (human, mouse) compared to PF-04457845 and URB597, which exhibited IC_{50} values of ~0.01 and 0.13 µM, respectively (Figure 5.1B), that generally matched previously reported results for these inhibitors.[6,20]

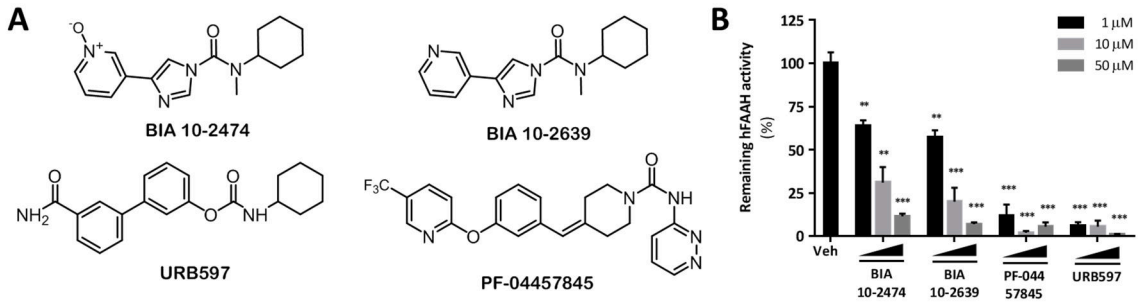

Figure 5.1 | Chemical structure and potency of human FAAH inhibitors. A) Structures of BIA 10-2474, metabolite BIA 10-2639, PF-04457845 and URB597. B) hFAAH activity relative to control after incubation with 1, 10 and 50 µM of indicated inhibitors as measured in a radiometric [^{14}C]-anandamide assay on purified recombinant hFAAH enzyme. Activity is expressed as mean ± SEM (n=3) with *P<0.05, ** P<0.01, *** P<0.001 (two-tailed *t*-test).

Activity-based protein profiling (ABPP) is used for rapid and efficient visualization of endogenous serine hydrolase activities in native biological samples.[13,15] Comparative and competitive gel-based ABPP studies were performed with two different activity-based probes: the broad-spectrum serine hydrolase-directed probe fluorophosphonate-rhodamine (FP-TAMRA)[15] and the tailored probe MB064 that preferentially reacts with endocannabinoid hydrolases diacylglycerol lipase-α (DAGL-α), α/β-hydrolase domain containing protein (ABHD) 6, and ABHD12, along with a handful of other enzymes.[14,17] Together, FP-TAMRA and MB064 provide target engagement assays for FAAH and a broad array of other brain serine hydrolases. As a first screen, a gel-based ABPP assay using mouse brain proteomes was performed. In total, 50 fluorescent bands were identified corresponding to putative serine hydrolases. Representative gel-based ABPP data are shown (Figure 5.2). The clinical trial subjects who developed neurological symptoms were exposed to a concentration of BIA 10-2474 that was 20 to 50 times higher than required for full blockade of FAAH activity.[4] Therefore, inhibitor activities against FAAH and other serine hydrolases were initially evaluated at two high concentrations (10 and 50 μM) in brain soluble and membrane proteomes. All tested compounds inhibited FAAH, with BIA 10-2474 showing the weakest activity, while also exhibiting distinctive off-target activities. In particular, BIA 10-2474 reduced the intensity of an additional fluorescent band in the membrane proteome (red box in panel A), which was identified as ABHD6 based on previous research.[16] PF-04457845 and URB597 reduced the fluorescent labeling of 2 other proteins, but ABHD6 was notably not among them. Moreover, BIA 10-2474 did not prevent labeling of the endocannabinoid hydrolases monoacylglycerol lipase (MAGL) or DAGL-α (Figure 5.2).

The brain target engagement profiles were confirmed and extended by performing ABPP coupled to high-resolution quantitative mass spectrometry (MS). This methodology allows for a more accurate quantification by avoiding band overlap (as observed with the gel-based assay) and enables screening over a broader range of specified serine hydrolases.[13] Mouse brain proteomes treated with inhibitor or vehicle were incubated with the serine hydrolase-directed activity-based probes FP-biotin and MB108, a biotinylated version of MB064. Probe-labeled enzymes were enriched by avidin chromatography, digested with trypsin, and the resulting tryptic peptides modified by reductive dimethylation (ReDiMe) of the NH_2-groups of N-termini and lysine residues using isotopically heavy and light formaldehyde. In these experiments, inhibited serine hydrolases were identified as enzymes exhibiting low heavy/light ratios. Quantitative MS confirmed complete inhibition of FAAH and validated ABHD6 as a major off-target of BIA 10-2474 and its metabolite, but not PF-04457845 (Figure 5.3). In addition to ABHD6, CES1c and ABHD11 were also identified as partial BIA 10-2474 off-targets in murine brain. PPME1 was identified as a potential, partial off-target for PF-04457845 with a heavy/light ratio < 0.5 (Figure 5.3).

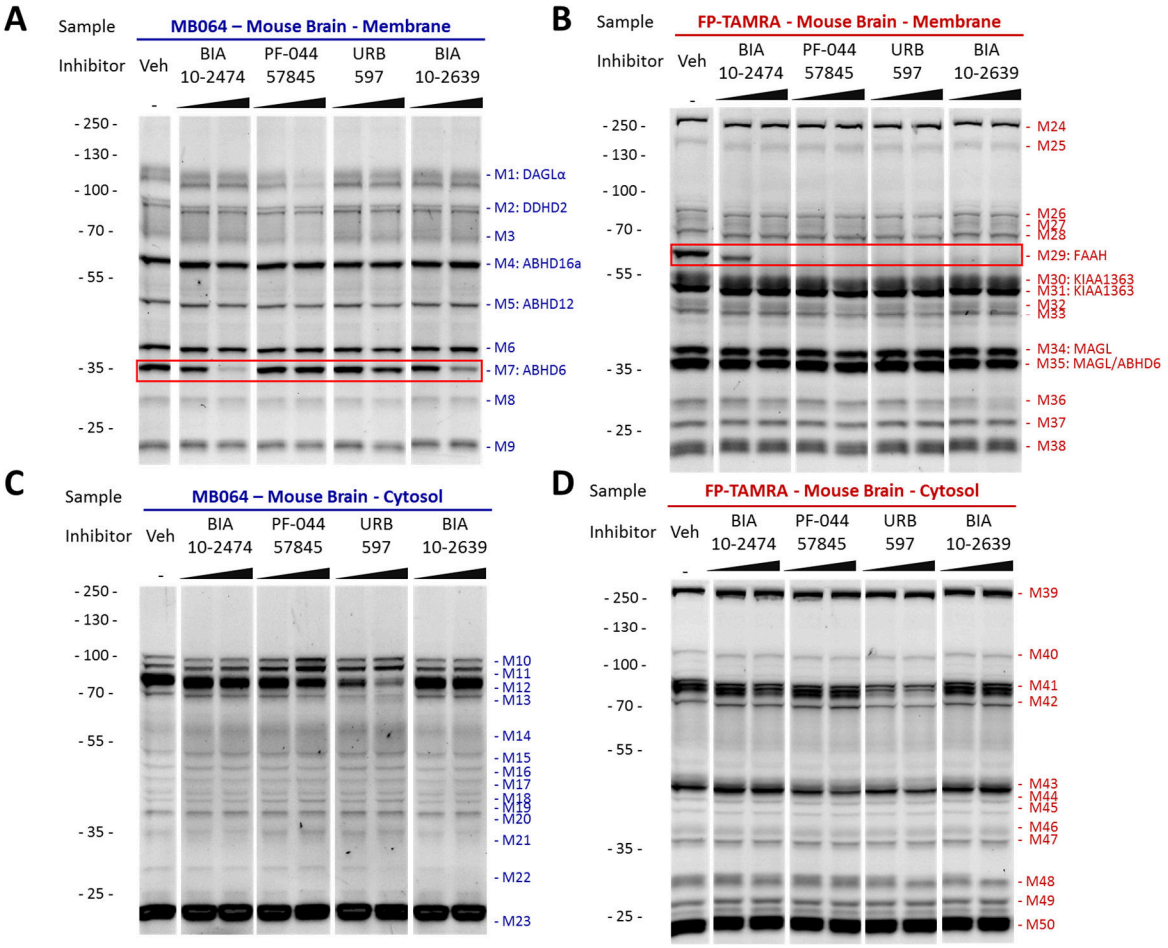

Figure 5.2| Identification of serine hydrolase targets of BIA 10-2474, PF-04457845, URB597 and BIA 10-2639 by competitive ABPP of mouse brain proteome. Mouse brain membrane (A, B) or cytosol (C, D) proteome was incubated with inhibitors (10 and 50 μM, 30 min, 37 ˚C) or DMSO as vehicle. Samples were incubated with MB064 (A,C) or FP-TAMRA (B,D). Red boxes highlight ABHD6 (A) and FAAH (B).

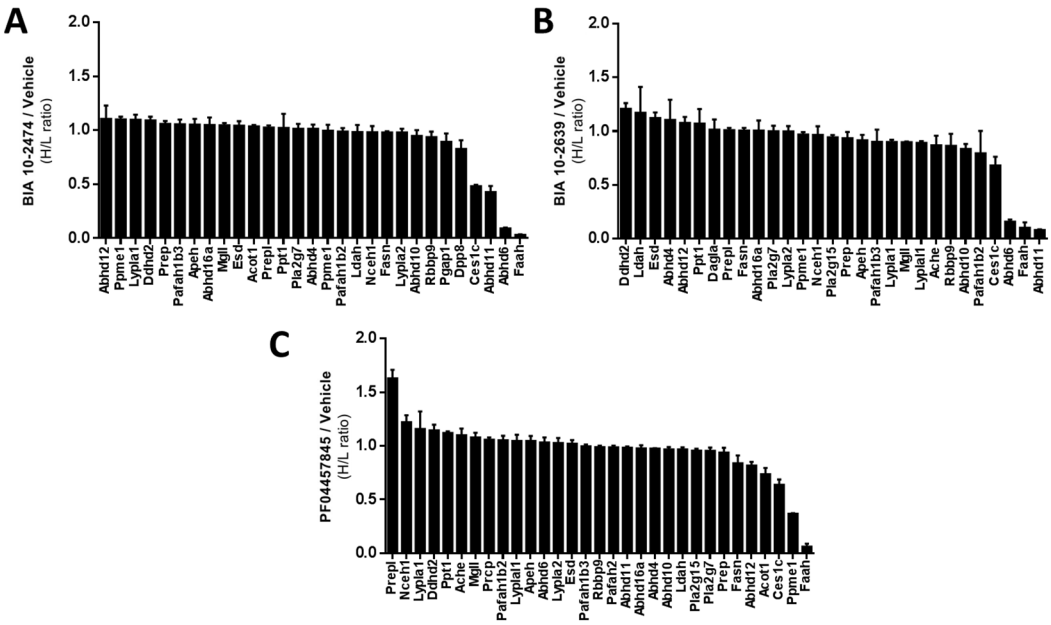

Figure 5.3 | MB108 and FP-biotin based chemoproteomic analysis of serine hydrolase activities in the mouse brain proteome treated with inhibitors BIA 10-2474 (A), BIA 10-2639 (B) and PF-04457845 (C) (50 μM, 30 min, 37 °C). Data is expressed as mean ± SEM (n=3).

Using dedicated activity and binding assays it was determined that BIA 10-2474 and PF-04457845 did not cross-react with other proteins of the endocannabinoid system, including cannabinoid CB_1 and CB_2 receptors, DAGL-α, DAGL-β, MAGL and *N*-acyl-phosphatidylethanolamine phospholipase D (NAPE-PLD), nor with the endocannabinoid-binding TRP ion channels (TRPV1-4, TRPM8 and TRPA1) (Supplementary Tables 1 and 2).

Finally, activity-based probes based on the structure of BIA 10-2474 were designed to identify potential non-serine hydrolase proteins that are directly modified by the inhibitor. To this end, compounds AJ167, AJ179 and AJ198 were synthesized (Figure 5.4), in which an alkyne functionality was introduced at different positions in BIA 10-2474. In all three probes, the alkyne group serves as a ligation handle to introduce fluorescent reporter groups via copper(I)-catalysed azide-alkyne cycloaddition ("click") chemistry.[21] Competitive ABPP revealed that compounds AJ179 and AJ198 are effective FAAH inhibitors and that ABHD6 can be partially inhibited by compounds AJ167 and AJ198 (Figure 5.5). Reaction of mouse brain proteomes treated with compound AJ167, AJ179, or AJ198 to a fluorophore using click chemistry revealed labeling of a band at the molecular weight of FAAH for probe AJ179 and AJ198. Additionally, compounds AJ179 and AJ198 also labeled a protein at the molecular weight of ABHD6. All FAAH and ABHD6 bands could be competed with BIA 10-2474. Importantly, these experiments definitively prove covalent binding of AJ179 and AJ198 to FAAH, which was maintained even under SDS-PAGE denaturing conditions. This observation, together with ~3-fold increased potency towards rat brain FAAH following a 20 min pre-incubation[22], supports an irreversible inhibition mechanism for BIA 10-2474. Few additional labeled proteins were detected, indicating that BIA 10-2474 has limited cross-reactivity with non-serine hydrolases in the brain proteome.

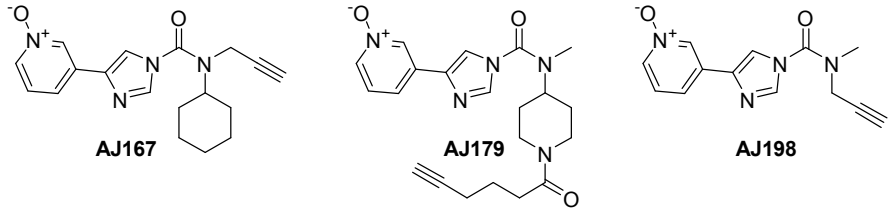

Figure 5.4 | Chemical structures of alkynylated BIA 10-2474-based probes AJ167, AJ179, and AJ198.

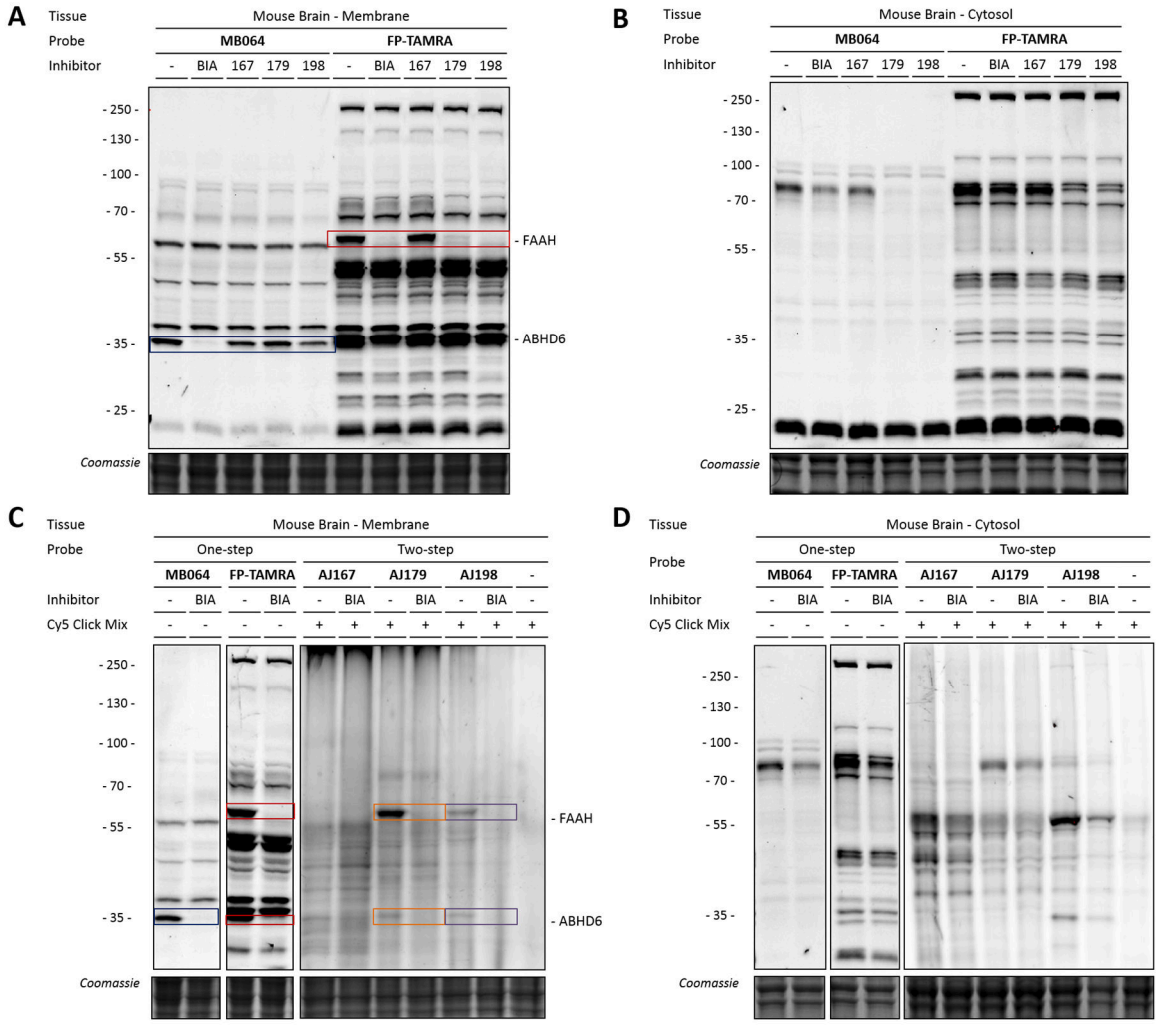

Figure 5.5 | Mouse brain membrane (A) or cytosol (B) proteomes were incubated with BIA 10-2474, the alkyne probes (50 µM, 30 min, 37 °C) or vehicle (DMSO). Residual activity was labeled with MB064 or FP-TAMRA. C-D) Mouse brain membrane (C) or cytosol (D) proteomes were incubated with BIA 10-2474 (50 µM, 30 min, 37 °C) or vehicle (DMSO). Samples were then incubated with alkyne probes (AJ167, AJ179 or AJ198; 50 µM, 30 min, 37 °C) or vehicle (DMSO), followed by a copper-catalyzed azide-alkyne cycloaddition to Cy5-azide. Competitive ABPP of BIA 10-2474 with MB064 or FP-TAMRA (as described for A, B) is shown as a reference.

As noted above, BIA 10-2474 exhibited weaker *in vitro* potency for FAAH compared to PF-04457845 and other advanced FAAH inhibitors. Remarkably, however, this difference was attenuated *in situ*, as gel-based ABPP experiments revealed that BIA 10-2474 inhibited FAAH, as well as other serine hydrolases (e.g., FAAH2, ABHD6) with substantially increased potency in human cells (Figure 5.6). The reason for the increased cellular activity of BIA 10-2474 is at present unclear, but it is not specific to one protein, which may suggest that cellular accumulation of the compound provides sufficiently high intracellular concentrations to inhibit FAAH and other serine hydrolases (*vide infra*).

In light of these data, the structural analogues AJ167, AJ176 and AJ198 were also expected to label more efficiently *in situ*. To test this hypothesis murine neuroblastoma (Neuro-2a) cells were treated with medium containing either BIA 10-2474, or either one of the three alkynated derivatives (Figure 5.7). From Figure 5.7A, it is clear that the two-step probes are much more efficient *in situ* (IS) than *in vitro* (IV). Especially AJ198 showed a

remarkable increase in labeling. Figure 5.7B shows a competition experiment between BIA 10-2474 and all three two-step probes. This demonstrated that the two bands shared by all probes were in fact FAAH and ABHD6 (red boxes) and these could be outcompeted by BIA 10-2474. All other clearly visible bands failed to be outcompeted. Therefore, it was decided not to pursue MS-based ABPP with these probes, because it is unlikely that this would yield additional off-targets.

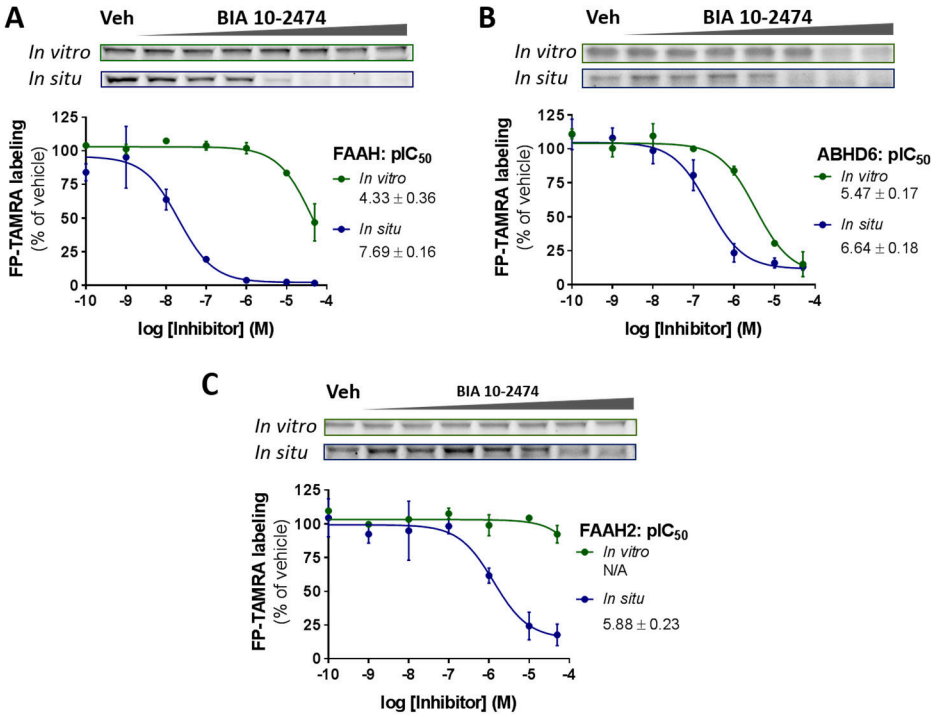

Figure 5.6 | HEK293T cells transiently overexpressing FAAH (A), endogenously expressing ABHD6 (B) and overexpressing FAAH2 (C) were treated with BIA 10-2474 (2 h, 37 °C) or DMSO as vehicle (n=3). Membrane fractions of untreated overexpressing cells were incubated with BIA 10-2474 (30 min, 37 °C) or DMSO as vehicle (*in vitro*). All samples were labeled with FP-TAMRA. Coomassie staining was used as loading control.

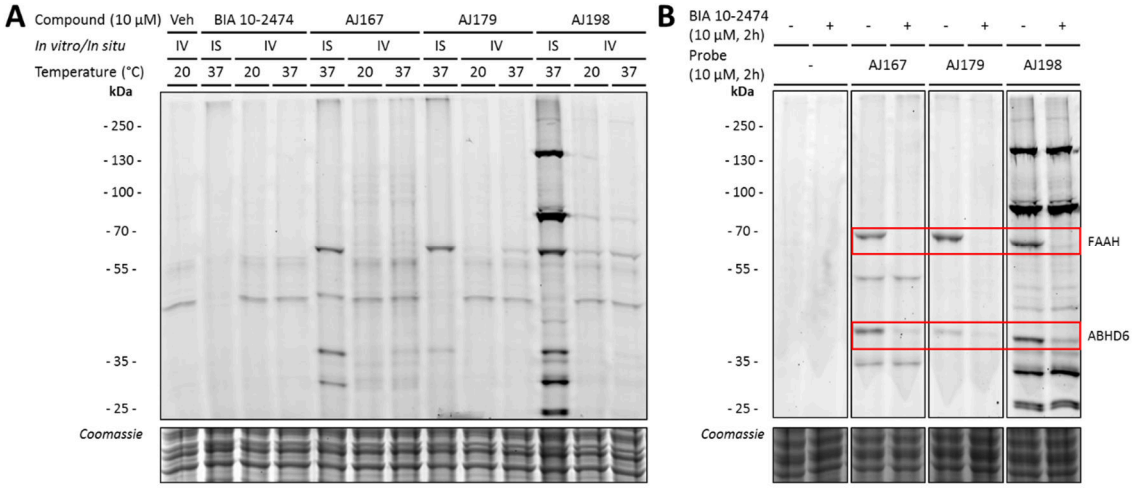

Figure 5.7 | *In situ* and *in vitro* activity profile of BIA 10-2474, AJ167, AJ179 and AJ198 by two-step competitive ABPP. Neuro-2a cells were treated *in situ* (IS) with BIA 10-2474, AJ167, AJ179 or AJ198 (10 µM, 2 h, 37°C) or *in vitro* (IV) with BIA 10-2474, AJ167, AJ179, AJ198 (10 µM, 30 min, 20/37°C) or vehicle (DMSO). Probe labeled targets were ligated to Cy5. Coomassie staining was used as a protein loading control.

The adverse effects observed during the clinical trial of BIA 10-2474 were not present in the preclinical toxicity profiling.[3] It was thus hypothesized that the off-target profile of BIA 10-2474 might also differ between species. Taking into account the potency difference between *in situ* versus *in vitro*, BIA 10-2474-treated cultured human neurons were profiled in ABPP studies. Several additional off-targets were identified: carboxyl esterase 2 (CES2), phospholipase 2 group XV (PLA2G15, also known as lysosomal phospholipase A2 (LPLA2)) and patatin-like containing phospholipase domain protein 6 (PNPLA6) (Figure 5.8) by means of chemical proteomics.

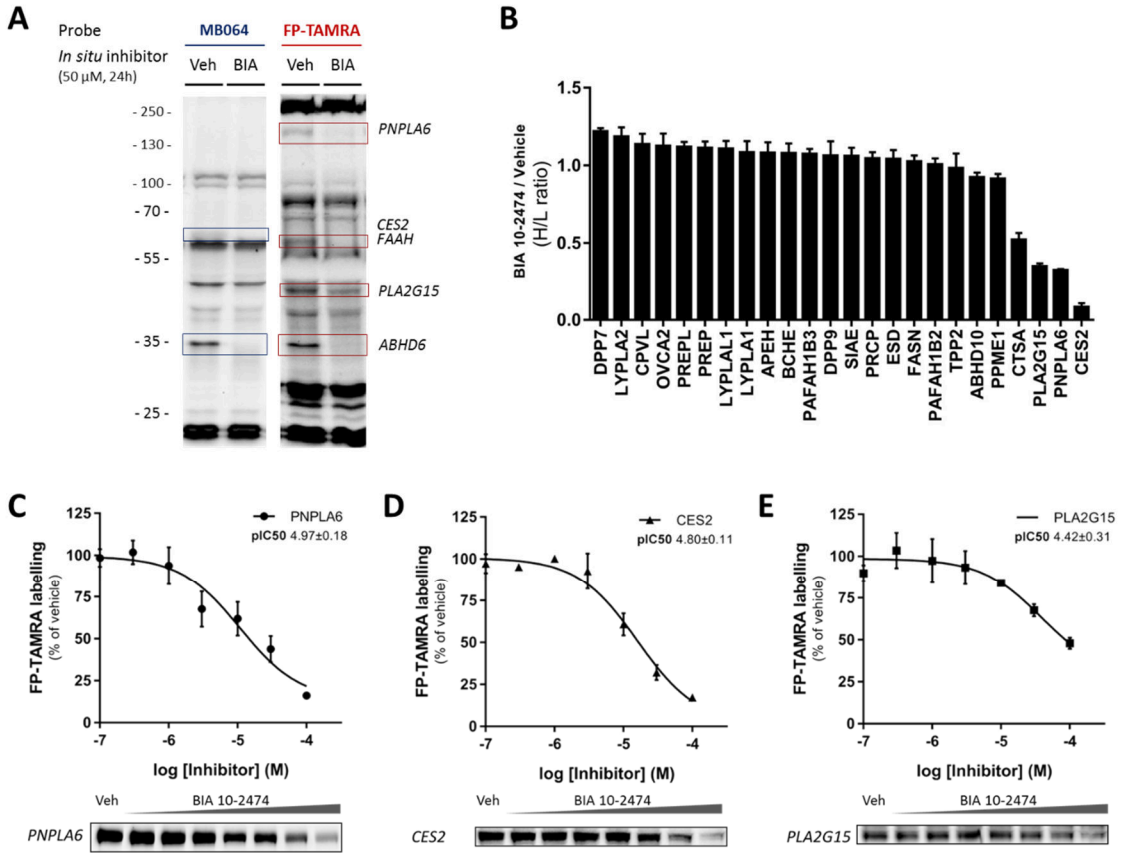

Figure 5.8 | *In situ* treatment of human neuronal cultures reveals additional BIA 10-2474 off-targets. A) Human neuronal cultures were treated *in situ* with BIA 10-2474 (50 µM, 24 h, 37 °C) or DMSO as vehicle (n=3). Lysates were incubated with FP-TAMRA or MB064. B) FP-biotin based chemoproteomic analysis of serine hydrolase activities in human neuronal cultures treated *in situ* with BIA 10-2474 or DMSO as vehicle (50 µM, 24 h, 37 °C). C-E) *In situ* dose response of BIA 10-2474 (0.1 - 100 µM, 24 h, 37 °C) and DMSO as vehicle on cells transiently overexpressing PNPLA6 (C), CES2 (D), and PLA2G15 (E). Data is expressed as mean ± SEM (n=3).

Most of the interaction partners of BIA 10-2474 identified in this study are involved in cellular lipid metabolism.[23–26] To confirm the interaction of BIA 10-2474 with lipolytic serine hydrolase off-targets, these human enzymes were transiently overexpressed in HEK293T cells. Concentration-dependent inhibition by BIA 10-2474 was assessed using gel-based ABPP (Figure 5.8C-E). BIA 10-2474 was found to inhibit PNPLA6, CES2 and PLA2G15 with IC_{50} values of 11, 16 and 38 µM, respectively. It is also noted that human CES2, as well as human ABHD6, were inhibited more potently by BIA 10-2474 and BIA 10-2639 than the mouse orthologues of these enzymes (data not shown). The found off-target profile led to the hypothesis that prolonged exposure to BIA 10-2474 might result in alterations of lipid metabolism in human cells. To test this hypothesis, targeted lipidomics analysis of human neuronal cultures treated with vehicle or BIA 10-2474 was performed. In total, 161 lipid species were quantified from which significant changes in several lipid classes were observed. Levels of *N*-acylethanolamines, triglycerides, monoacylglycerols and (lyso)phosphatidylcholines were increased in BIA 10-2474-treated cells, while those of free fatty acids and plasmalogens were reduced (Figure 5.9A). Notably, these alterations in cellular lipid metabolism are consistent with the inhibition of FAAH, FAAH2, ABHD6, CES2, PLA2G15 and PNPLA6 activities. Neuronal cells treated with PF-04457845 (1 µM) only showed significant increase in the *N*-acylethanolamine levels, consistent with selective FAAH inhibition (Figure 5.9B).

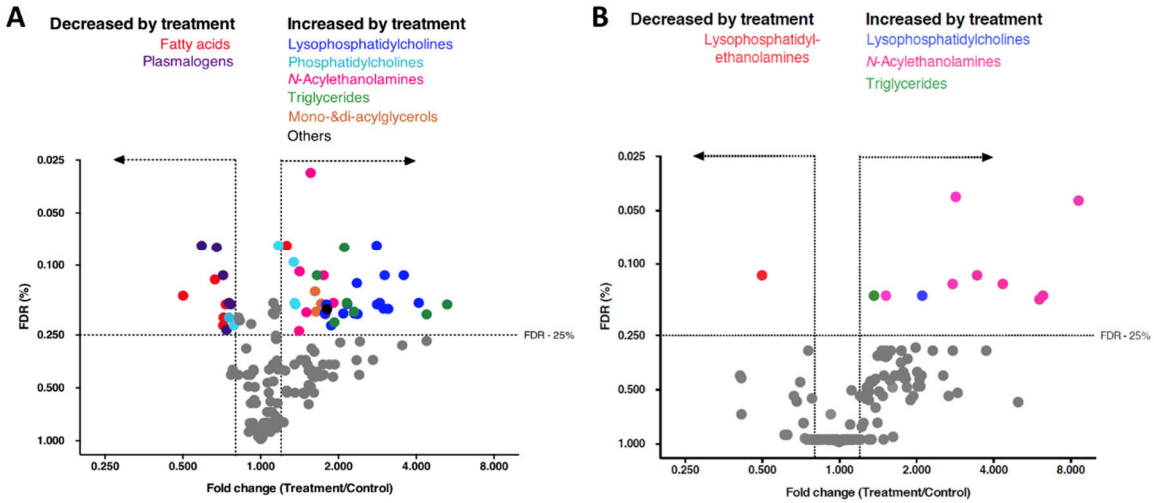

Figure 5.9 | Volcano plot of lipidomic analysis of human neurons treated *in situ* with BIA 10-2474 (50 µM, 48 h, 37 °C) (A) and PF-04457845 (1 µM, 48 h, 37 °C) (B) compared to cells treated with DMSO as vehicle. Lipids with a fold change (FC) threshold of ≥1.20 or ≤0.80 and Benjamini–Hochberg false discovery rate (FDR) ≥ 25% are represented by coloured circles distinguished by lipid class. Based on average lipid levels (n=3)

Discussion

Severe adverse effects of drug candidates are rarely observed in phase 1 clinical trials, due to extensive preclinical toxicological profiling in animals and precautions taken into account in the design of first-in-human studies.[1] No obvious toxicological results in rodents were found that could predict the observed human clinical neurotoxicity. In a study on dogs treated for 13 weeks with BIA 10-2474, a dose-dependent pulmonary toxicity was observed and two dogs from the subgroup receiving the highest dose were sacrificed. An initial toxicology study in primates showed that the highest administered dose led to axonal dystrophy in the spinal bulb. A follow-up primate study led to the death of one animal and the sacrifice of several others for undisclosed ethical reasons. These findings were not, however, considered to be sufficiently concerning to abandon the first-in-human studies due to the large therapeutic window in preclinical studies of BIA 10-2474.[4]

The main remaining hypothesis to explain the human clinical neurotoxicity of BIA 10-2474 as put forward by the French authorities[4] (i.e. off-target activity of BIA 10-2474 and/or its metabolites) was the basis of the here described study. BIA 10-2474 was shown to be an irreversible, potent FAAH and FAAH2 inhibitor that increases cellular levels of long-chain fatty acid ethanolamides. Using ABPP with mouse brain proteomes and human cortical neuron proteomes, BIA 10-2474, but not PF-04457845, was found to inhibit multiple lipases, including ABHD6, CES2, PLA2G15 and PNPLA6. BIA 10-2474 also disrupted neural lipid metabolism as witnessed by increased levels of *N*-acylethanolamines, monoacylglycerols, triglycerides phosphatidylcholine, (lyso)phosphatidylcholine, and reductions in free fatty acids and plasmalogens. When considering the basis for BIA 10-2474's broader interaction profile with serine hydrolases compared to PF-04457845, it is suspected that the greater intrinsic reactivity of BIA 10-2474 may be a contributing factor, though this warrants further investigation.

FAAH2 is a human-specific orthologue of FAAH, which also degrades long-chain fatty acid amides.[27] However, little is known about the neurobiological function of FAAH2. CES2 is a serine esterase involved in the hydrolysis of ester and amide bonds of xenobiotics and prodrugs, but also of endogenous lipids. It is highly expressed in the liver and in endothelial cells. Hepatic CES2 is required for triglyceride homeostasis by modulating lipolysis, ER stress and lipogenesis.[28] PLA2G15 is a lysosomal phospholipase highly expressed in alveolar macrophages and microglial cells. Inhibition of PLA2G15 leads to accumulation of phosphatidylcholines and phosphatidylethanolamines, and has previously been implicated in drug-induced phospholipidosis.[25]

PNPLA6 (also known as neuropathy target esterase, NTE) has previously been linked to neurodegeneration in humans resulting from exposure to organophosphate-based pesticides.[24,29] PNPLA6 is a (lyso)phospholipase that uses (lyso)phosphatidylcholine as a substrate and is highly expressed in endothelial cells, astrocytes and neurons. Proper neuronal phosphatidylcholine homeostasis mediated by PNPLA6 is required for axonal maintenance.[30] PNPLA6 inhibition leads to neurodegeneration following an age-dependent neuropathy of increasing severity in older age. Notably, PNPLA6-mediated neurotoxicity following acute organophosphate exposure is species dependent, with less pronounced effects in rodents than humans. Mice with a homozygous germline deletion of PNPLA6 have embryonic lethality due to placental and vasculature defects, however, brain-specific

deletion of PNPLA6 results in prominent neuronal pathology.[31] A threshold of >70% PNPLA6 inhibition has been determined as responsible for developing neurodegeneration upon organophosphate exposure in chicken.[24,29] In the light of this data, it is remarkable that many clinical symptoms arising from PNPLA6-mediated neurological sequelae following organophosphate exposure resemble the neuropathology observed in the clinical trial participants who received a cumulative dose of 250-300 mg of BIA 10-2474, including precedent for human neurotoxicity, brain region sensitivity, age dependency, species selectivity, dosing threshold and time course of neuropathology. However, while our data provide information about the selectivity of BIA 10-2474, they do not allow us to conclude that inhibition of one or more of the identified off-target proteins is responsible for the clinical neurotoxicity caused by this drug. Nor can we exclude the possibility that non-covalent interactions of BIA 10-2474 or its metabolites with other proteins might have contributed to the reported clinical effects.[32]

Regardless, our study highlights the general utility of ABPP as a versatile chemical proteomic method to assess on-target engagement and off-target activity of covalent drugs to guide therapeutic development.

Acknowledgements

Maaike Bril is kindly acknowledged for her work regarding the *in situ* profiling of the alkynated BIA 10-2474 analogues.

Methods

Probes and inhibitors

Activity based probe TAMRA-fluorophosphonate (FP-TAMRA) was purchased from Thermo Fisher, MB064 was synthesized in-house as previously described.[14] PF-04457845 was synthesized in house and purchased from Sigma Aldrich. URB597 was purchased from Sigma Aldrich. Inhibitor BIA 10-2474, BIA 10-2639 and activity based probes AJ167, AJ179 and AJ198 were synthesized as described in the synthetic methods *(vide infra)*. All synthesized compounds were at least 95% pure and were analyzed by LC/MS, NMR and HRMS. Other chemicals, reagents, and primers were purchased from Sigma Aldrich unless indicated otherwise.

Cloning

Full-length human cDNA of ABHD6, FAAH, ABHD11, PNPLA6, CES2 (Source Bioscience) and FAAH2 (BioCat) was cloned into mammalian expression vector pcDNA3.1, containing genes for ampicillin and neomycin resistance. The inserts were cloned in frame with a C-terminal FLAG-tag and site-directed mutagenesis was used to remove restriction by silent point mutations. Plasmids were isolated from transformed XL-10 Z-competent cells (Maxi Prep kit: Qiagen) and sequenced at the Leiden Genome Technology Center. Sequences were analyzed and verified (CLC Main Workbench).

Cell culture

General

HEK293T (human embryonic kidney) and Neuro-2a (mouse neuroblastoma) cells were cultured at 37 °C under 7% CO_2 in DMEM containing phenol red, stable glutamine, 10% (v/v) New Born Calf Serum (Thermo Fisher), and penicillin and streptomycin (200 µg/mL each; Duchefa). Medium was refreshed every 2-3 days and cells were passaged twice a week at 80-90% confluence by resuspension in fresh medium.
Cells lines were purchased from ATCC and were regularly tested for mycoplasma contamination. Cultures were discarded after 2-3 months of use.

Human neural cell culture

Human iPSC-derived neural progenitor cells (NPCs) (Axol Biosciences, line ax0015) were plated on sterile coverslips in 12-well plates, coated with poly-L-ornithin/laminin (Sigma-Aldrich), in neural differentiation medium (Neurobasal medium, 1% N2 supplement, 2% B27-RA supplement, 1% MEM-NEAA, 20 ng/mL BDNF (ProSpec Bio)), 20 ng/mL GDNF (ProSpec Bio), 1 µM db-cAMP (Sigma-Aldrich), 200 µM ascorbic acid (Sigma-Aldrich), 2 µg/mL laminin, and 1% P/S), resulting in neural networks composed of neurons and glia. Cells were refreshed with neural differentiation medium 3 times per week. During weeks 1-4, medium was fully refreshed. After 4 weeks of neural differentiation, only half of the volume of medium per well was refreshed.

Transient transfection

One day prior to transfection HEK293T cells were seeded to 15-cm dishes or 12-well plates (~62.500 cells/cm^2). Prior to transfection, culture medium was aspirated and a minimal amount of medium was added. A 3:1 (m/m) mixture of polyethyleneimine (PEI) (60 µg/dish or 1.875 µg/well) and plasmid DNA (20 µg/dish or 0.625 µg/well) was prepared in serum-free culture medium and incubated for 15 min at RT. Transfection was performed by dropwise addition of the PEI/DNA mixture to the cells. Transfection with the empty pcDNA3.1 vector was used to generate control samples. After 24 h, medium was refreshed. Medium was aspirated 48 or 72 h post-transfection and cells were harvested by resuspension in PBS. Cells were pelleted by centrifugation (5 min, 1,000 *g*) and the pellet was washed with PBS. Supernatant was discarded and cell pellets were frozen in liquid nitrogen and stored at -80 °C until sample preparation.

In situ treatment of HEK293T or Neuro-2a cells

In situ treatment was initiated 24 h (for 24 – 48 h treatment) or 48 h (for 2 h treatment) post-transfection in 12-well plates. Medium was aspirated and medium containing inhibitor or DMSO as vehicle was added (0.1-1.0% v/v DMSO, DMSO concentration constant within each experiment). Final concentrations for inhibitors are indicated in the main text and figure legends. After 2, 4, 24, or 48 h exposure to treatment medium, medium was aspirated and cells were harvested and stored as described above until sample preparation (whole cell lysate).

In situ treatment of human neural cell culture

Cells were treated with inhibitor *in situ* 7-8 weeks after plating of NPCs. Culture slides were then collected from 6-well culture plates 24 h or 48 h after initiation of *in situ* treatment with BIA 10-2474 (50 µM, 0.25% DMSO) or vehicle (0.25% DMSO). The *in situ* treated cells were harvested in PBS as described above and stored at -80 °C until further use.

Sample preparation

Whole cell lysate

Cell pellets were thawed on ice, resuspended in cold lysis buffer (20 mM HEPES, pH 7.2, 2 mM DTT, 250 mM sucrose, 1 mM $MgCl_2$, 2.5 U/mL benzonase) and incubated on ice (15-30 min). The cell lysate was used for membrane preparation (below) or diluted to appropriate concentration in cold storage buffer (20 mM Hepes, pH 7.2, 2 mM DTT) for use as whole lysate (HEK293T: 2.0 mg/mL, human cortical neurons: 0.75 mg/mL, human neural cells: 1.5 mg/mL). Protein concentrations were determined by a Quick Start™ Bradford Protein Assay and diluted samples were flash frozen in liquid nitrogen and stored at -80 °C until further use.

Tissue lysate

Mouse brains (C57Bl/6) were isolated according to guidelines approved by the ethical committee of Leiden University (DEC#13191), frozen in liquid nitrogen, and stored at -80 °C until use. Tissues were thawed on ice, dounce homogenized in cold lysis buffer and incubated on ice (15 min), followed by two low-speed spins (3 min, 1,400−2,500 *g*, 4 °C) to remove debris. The supernatant fraction was collected for further use.

Membrane preparation from lysate

The membrane and cytosolic fractions of cell or tissue lysates were separated by ultracentrifugation (93,000 *g*, 45 min, 4°C). The supernatant was collected (cytosolic fraction) and the membrane pellet was resuspended in cold storage buffer by thorough pipetting and passage through an insulin needle. Protein concentrations were determined by a Quick Start™ Bradford Protein Assay and samples were diluted to 2.0 mg/mL with cold storage buffer, flash frozen in liquid nitrogen and stored at -80 °C until further use. FAAH and FAAH2 overexpression membranes were mixed in an appropriate ratio for ABPP (0.1 mg/mL: 1.0 mg/mL).

Activity based protein profiling

Gel based: Direct activity based probes

Gel-based ABPP was performed and analyzed with minor adaptations on previously reported procedures.[14] In brief, for *in vitro* inhibition, or mouse brain proteome or cell lysate (15 µL, 0.75, 1.5 or 2.0 mg/mL, lysate, cytosol or membrane fraction) was pre-incubated with vehicle or inhibitor (0.375 µL 40* inhibitor stock, 30 min, 37 °C) followed by an incubation with the activity-based probe (0.375 µL 40* stock, final concentrations: 250 nM for MB064 or 500 nM for FP-TAMRA, 20 min, RT). Final concentrations for the inhibitors are indicated in the main text and figure legends. For *in situ* inhibition, the *in situ*-treated cells (15 µL whole lysate) were directly incubated with the activity-based probe (0.375 µL 40* stock, final concentrations: 250 nM for MB064 or 500 nM for FP-TAMRA, 20 min, RT). Reactions were quenched with 4* Laemmli buffer (5 µL, 240 mM Tris (pH 6.8), 8% (w/v) SDS, 40% (v/v) glycerol, 5% (v/v) β-mercaptoethanol, 0.04% (v/v) bromophenol blue). 7.5, 15 or 20 µg per reaction was resolved on a 10% acrylamide SDS-PAGE gel (180 V, 75 min). Gels were scanned using Cy3 and Cy5 multichannel settings (605/50 and 695/55, filters respectively) and stained with Coomassie after scanning. Fluorescence was normalized to Coomassie staining and quantified with Image Lab (Bio-Rad). IC_{50} curves were fitted with Graphpad Prism® 7 (Graphpad Software Inc.).

Gel based: Two-step activity based probes

The two-step labeling protocol was adapted from previously developed methods.[33] In brief, human or mouse proteome (40 µL, 2 mg/mL, cytosol or membrane fraction) was pre-incubated with vehicle (DMSO) or inhibitor (50 µM, 30 min, 37 °C) followed by an incubation with the alkyne probe (50 µM, 30 min, 37 °C). Click reagent was freshly prepared by mixing copper sulfate (2 µL/reaction, 100 mM in water), THPTA (0.4 µL/reaction, 100 mM in water), sodium ascorbate (1.2 µL/reaction, 1 M in water), and Cyanine 5-Azide (Cy5−N_3, 1.60 µL/reaction, 1 mM in DMSO). Click reagent (5.0 µL) was added to each proteome, mixed by brief vortexing and incubated (60 min, RT). Proteins were precipitated by adding methanol (50 µL), chloroform (15 µL) and water (15 µL), mixed by brief vortexing and pelleted by centrifugation (10 min, 4000 rpm). The supernatant was removed and the pellet was washed twice with methanol (50 µL). The pellet was then redissolved in 40 µL

of 2* Laemmli buffer (120 mM (pH 6.8), 4% (w/v) SDS, 20% (v/v) glycerol, 2.5% (v/v) β-mercaptoethanol, 0.02% (v/v) bromophenol blue) by vortexing. Samples were boiled (95 °C, 5 min) and 20 µg proteome per reaction was resolved on a 10% acrylamide SDS-PAGE gel (180 V, 75 min). Gels were scanned using Cy3 and Cy5 multichannel settings (605/50 and 695/55, filters respectively) and stained with Coomassie after scanning. Coomassie staining was performed as a protein loading control.

Activity-based proteomics

Activity-based proteomics was based on previously described procedures.[17] In summary, mouse whole brain proteome (250 µL cytosolic or membrane fraction at 1.0 mg/mL) was incubated with vehicle (2% DMSO) or inhibitor (BIA 10-2474**,** BIA 10-2639, or PF-04457845, 50 µM, 30 min, 37 °C). The proteome of *in situ* treated human neural cells (250 µL whole lysate at 0.35 mg/mL, 24 h treatment) was used without additional inhibitor incubation. The proteomes were then labeled with MB108 or FP-Biotin (10 µM, 60 min, RT). The labeling reaction was quenched and excess probe was removed by chloroform methanol precipitation. Precipitated proteome was resuspended in 6 M Urea/25 mM ammonium bicarbonate (250 µL) and incubated (15 min, RT). Subsequently DTT (2.5 µL, 1 mM) was added and the mixture was incubated (15 min, 65 °C). The sample cooled to RT and iodoacetamide (0.5 M, 20 µL) was added to alkylate the sample (30 min, RT, dark). SDS (70 µL, 10% (v/v)) was added and the proteome was heated (5 min, 65 °C). The sample was diluted with PBS (3 mL). 50 µL of a 50% slurry of Avidin−Agarose from egg white (Sigma-Aldrich) was washed with PBS and added to the proteome sample. The beads were incubated with the proteome (3 h, RT, shaking). The beads were isolated by centrifugation (2500 *g*, 2 min) and washed with SDS in PBS (10 mL, 0.5% (w/v)), followed by 3 washes with PBS. The beads were transferred to low-binding Eppendorf tubes and proteins were digested with sequencing grade trypsin (Promega) (500 ng per sample) in 250 µL buffer (100 mM Tris, 100 mM NaCl, 1 mM $CaCl_2$, 2 % acetonitrile) (37 °C, O/N, vigorous shaking). The pH was adjusted with formic acid to pH 3 and the beads were removed by filtration.

The peptides were isotopically labeled by on stage tip dimethyl labeling according to literature procedures[17], with the following modification. Dimethyl labeling was performed by the subsequent addition of 20, 20, 30, 30 and 40 µL of Light (vehicle) or Medium (inhibitor) reagent to the stage tips. The centrifugation speed during labeling was adjusted to have a flow through time of approximately 5 min (400-1000 *g*) per labeling step.

Targeted lipidomics

Sample extraction

Lipids were extracted from *in situ* treated human neural cells (48 h, 50 µM BIA 10-2474 or vehicle (0.25% DMSO)). The sample extraction was performed on ice. In brief, cell pellets with 1 million cells were transferred to 1.5 mL Eppendorf tubes, spiked with 10 µL each of deuterated labeled internal standard mix for endocannabinoids (*N*-arachidonoyl ethanolamine (AEA)-d8, *N*-arachidonoyldopamine (NADA)-d8, *N*-docosahexaenoylethanolamide (DHEA)-d4, 2-arachidonoylglycerol (2-AG)-d8, *N*-stearoylethanolamine (SEA)-d3, *N*-palmitoylethanolamine(PEA)-d4, *N*-linoleoylethanolamine (LEA)-d3 and *N*-oleoylethanolamine (OEA)-d4), positive apolar lipids (lysophosphatidylcholines (LPC)17:0, phosphatidylethanolamines (PE)17:0/17:0, phosphatidylcholines (PC)17:0/17:0, sphingomyelins (SM) d18:1/17:0, triglycerides (TG) 17:0/17:0/17:0, ceramides (Cer) d18:1/17:0) and negative polar lipids (fatty acid (FA)17:0-d33), followed by the addition of ammonium acetate buffer (100 µL, 0.1 M, pH 4). After extraction with methyl *tert*-butyl ether (1 mL), the tubes were thoroughly mixed for 4 min using a bullet blender at medium speed (Next Advance, Inc., Averill park, NY, USA), followed by a centrifugation step (5000 *g*, 12 min, 4 °C). Then 925 µL of the upper layer methyl *tert*-butyl ether was transferred into clean 1.5 mL Eppendorf tubes. Samples were dried in a speed-vac followed by reconstitution in acetonitrile:water (50 µL, 90:10, v/v). The reconstituted samples were centrifuged (14,000 *g*, 3 min, 4 °C) before transferring into LC-MS vials. Each sample was injected on three different lipidomics platforms: endocannabinoids (5 µL), positive apolar lipids (2 µL) and for negative polar lipids (8 µL).

LC-MS/MS Analysis for endocannabinoids

A targeted analysis of 21 endocannabinoids and related NAEs (*N*-acylethanolamines) were measured using an Acquity UPLC I class Binary solvent manager pump (Waters, Milford, USA) in conjugation with AB SCIEX 6500 quadrupole-ion trap (QTRAP) (AB Sciex, Massachusetts, USA). Separation was performed with Acquity HSS T3 column (1.2 x 100 mm, 1.8 µm) maintained at 45 °C. The aqueous mobile phase A consisted of 2 mM ammonium formate and 10 mM formic acid, and the organic mobile phase B was acetonitrile. The flow rate was set to 0.4 mL/min; initial gradient conditions were 55% B held for 2 min and linearly ramped to 100% B over 6 minutes and held for 2 minutes; after 10 s the system returned to initial conditions and held 2 min

before next injection. Electrospray ionization-MS was operated in positive mode for measurement of 21 endocannabinoids and NAEs, and a selective Multiple Reaction Mode (sMRM) was used for quantification.

LC-MS/MS analysis for positive apolar and negative polar lipids

Both lipidomics methods are adapted and modified from previously published work.[34] Briefly, these methods are measured on an Acquity UPLC Binary solvent manager pump (Waters) coupled to an Agilent 6530 electrospray ionization quadrupole time-of-flight (ESI-Q-TOF, Agilent, Jose, CA, USA) high resolution mass spectrometer using reference mass correction. The chromatographic separation was achieved on an Acquity HSS T3 column (1.2 x 100 mm, 1.8 µm) maintained at 40 °C for both methods. The positive polar lipids that include targets from different lipid classes including (lyso)phosphatidylcholines, triglycerides, ceramides. (lyso)phosphatidylethanolamines and sphingomyelins were separated using a flow of 0.4 mL/min over a 16 min gradient. In positive mode, the aqueous mobile phase A consisted of 60:40 (v/v) acetonitrile:H_2O with 10 mM ammonium formate, and the organic mobile phase B consisted of 10:90 (v/v) acetonitrile:isopropanol with 10 mM ammonium formate. The negative apolar lipids that constitute mainly free fatty acids and (lyso)phosphatidylcholines were separated with a flow of 0.4 mL/min over 15 min gradient. In negative mode, the aqueous mobile phase A consisted of 5:95 (v/v) acetonitrile:H_2O with 10 mM ammonium formate, and the organic mobile phase B consisted of 99% (v/v) methanol with 10 mM ammonium formate. The targets in both lipid methods were detected full scan (100-1000 m/z) in their respective ion charge mode.

Activity assays

Radiolabeled natural substrate assay hFAAH and mFAAH

The radiolabeled natural substrate based assay for human and mouse FAAH was performed as reported previously.[35] In brief, chemicals were of the purest analytical grade. Anandamide (AEA) was purchased from Sigma Chemical Co. (St. Louis, MO, USA). URB597 and purified hFAAH were obtained from Cayman Chemical (Ann Arbor, MI, USA). [^{14}C-ethanolamine]-anandamide (60 Ci/mmol) was purchased from ARC (St. Louis, MO). Mouse brain membranes (50 µg per test), prepared as reported[35], or hFAAH (2.5 µg per test) were pre-incubated for 15 min at room temperature with each compound, then they were incubated with 10 µM [^{14}C-ethanolamine]anandamide (15 min, 37 °C, in 500 µL of 50 mM Tris–HCl buffer (pH = 9)). The reaction was stopped by the addition of 0.6 mL of ice-cold methanol/chloroform (2:1, v/v). The mixture was centrifuged (3000 *g*, 5 min), the upper aqueous layer was put in a vial containing liquid scintillation cocktail (Ultima Gold XR, Perkin Elmer Life Sciences), and radioactivity was quantified in a β-counter.

Natural substrate-based fluorescence assay DAGL-α/β

The natural DAG substrate assay was performed as reported previously.[36] Standard assay conditions: 0.2 U/mL glycerol kinase (GK), glycerol-3-phosphate oxidase (GPO) and horseradish peroxidase (HRP), 0.125 mM ATP, 10 µM Amplifu™Red, 5% DMSO in a total volume of 200 µL. The assay additionally contained 5 µg/mL MAGL-overexpressing membranes, 100 µM SAG and 0.0075% (w/v) Triton X-100, with a final protein concentration of 50 µg/mL. The mDAGL-β assay was performed as the hDAGL-α assay, but assay buffer was supplemented with 5 mM $CaCl_2$ and the SAG concentration was 75 µM.

Natural substrate-based fluorescence assay MAGL

The natural substrate MAGL assay was performed as previously published.[36]

Surrogate substrate assay NAPE-PLD

The surrogate substrate assay was based on a previously reported method.[37] The membrane protein fraction HEK293T cells transiently overexpressing NAPE-PLD was diluted to 0.4 mg/mL in assay buffer (50 mM Tris-HCl (pH 7.5), 0.02% Triton X-100, 150 mM NaCl). The substrate PED6 (Invitrogen) stock (10 mM) was consecutively diluted in DMSO (25x) and in assay buffer (10x). Relevant concentrations of compounds were prepared in DMSO. The assay was performed in a dark Greiner 96 wells plate, end volume 100 µL. The membrane protein lysate (final concentration 0.04 mg/mL) was incubated with inhibitor or vehicle (30 min, 37 °C). A sample without membrane protein lysate was incorporated for background subtraction. Subsequently, substrate was added (PED6, final concentration: 1 µM) and the measurement was started immediately on a TECAN infinite M1000 pro (37 °C, scanning at 2 min intervals for 1 h: excitation 485 nm, emission 535 nm).

Radioligand displacement assays CB_1/ CB_2-receptor

[^{3}H]CP55940 displacement assays to determine the affinity for the cannabinoid CB_1 and CB_2 were performed as previously described[16,38], with the following changes: ligands of interest were incubated (25 °C, 2 h) with membrane aliquots containing 1.5 µg (CHOK1hCB_2_bgal) membrane protein in 100 µL assay buffer (50 mM Tris–HCl, 5 mM $MgCl_2$, 0.1 % BSA, pH 7.4) with ~1.5 nM [^{3}H]CP55940 per assay point. Non-specific binding was determined in the presence of 10 µM AM630. Filtration was performed on 96-well GF/C filters, each well presoaked for 30 min with 25 µL 0.25 % PEI, using a 96-wells Filtermate harvester (PerkinElmer). Filter-bound radioactivity was determined by scintillation spectrometry using a Microbeta® 2450 microplate counter (PerkinElmer).

Fluorescent Ca^{2+} assays for TRP ion channels

HEK293 (human embryonic kidney) cells stably over-expressing recombinant human TRPV1 or rat TRPA1, TRPV2, TRPV3, TRPV4, or TRPM8 were grown on 100 mm diameter Petri dishes as mono-layers in minimum essential medium (MEM) supplemented with non-essential amino acids, 10 % fetal bovine serum, 2 mM glutamine, and maintained at 5 % CO_2 at 37 °C. Quantitative real time analysis was carried out to measure TRP gene over-expression in transfected-cells (data not shown). On the day of the experiment, cells were loaded with the methyl ester Fluo-4 AM in MEM (4 µM in DMSO containing 0.02 % Pluronic F-127, Invitrogen), kept in the dark at room temperature for 1 h, washed twice with Tyrode's buffer (145 mM NaCl, 2.5 mM KCl, 1.5 mM $CaCl_2$, 1.2 mM $MgCl_2$, 10 mM D-glucose, and 10 mM HEPES, pH 7.4), resuspended in the same buffer and transferred (about 100,000 cells) to the quartz cuvette of the spectrofluorimeter (PerkinElmer LS50B equipped with PTP-1 Fluorescence Peltier System; PerkinElmer Life and Analytical Sciences, Waltham, MA, USA) under continuous stirring. The effects on intracellular Ca^{2+} concentration ($[Ca^{2+}]_i$) before and after the addition of various concentrations of test compounds was measured by cell fluorescence (λ_{EX} = 488 nm, λ_{EM} = 516 nm) at 25 °C. The effects of compounds were normalized against the response to ionomycin (4 µM) in each experiment. The increases in fluorescence in wild-type HEK293 cells (i.e. not transfected with any construct) were used as baseline and subtracted from the values obtained from transfected cells. Efficacy was defined as the maximum response elicited by the compounds tested and was determined by comparing their effect with the analogous effect observed with 4 µM ionomycin (Cayman), while the potency of the compounds (EC_{50}) was determined as the concentration required to produce half-maximal increases in $[Ca^{2+}]_i$. Curve fitting (sigmoidal dose–response variable slope) and parameter estimation were performed with GraphPad Prism® (GraphPad Software Inc., San Diego, CA).

Antagonist/desensitizing behavior was evaluated by adding the test compounds in the quartz cuvette 5 min before stimulation of cells with agonists. In the case of human TRPV1-expressing HEK293 cells the agonist used was capsaicin (0.1 µM, in the case of SR141716A 10 nM was also used), which was able of elevating intracellular Ca^{2+} with a potency of EC_{50} = 5.3 ± 0.4 nM and efficacy = 78.6 ± 0.6 %.

For TRPV2, the rat TRPV2-HEK293 cells exhibited a sharp increase in $[Ca^{2+}]_i$ upon application of lysophosphatidylcholine (LPC) 3 µM. The concentration for half-maximal activation was 3.40 ± 0.02 µM and efficacy was 91.7 ± 0.5 %.

In the case of TRPV3, rat TRPV3-expressing HEK-293 cells were first sensitized with the non-selective agonist 2-aminoethoxydiphenyl borate (100 µM). Antagonist/desensitizing behavior was evaluated against thymol (100 µM), which showed an efficacy of 34.7 ± 0.2 % and a potency of EC_{50} = 84.1 ± 1.6 µM. In the case of rat TRPV4-expressing HEK293 cells the agonist used was GSK1016790A, (10 nM), which was able of elevating intracellular Ca^{2+} with a potency of EC_{50} = 0.46 ± 0.07 µM, and an efficacy of 51.9 ± 1.7 %. In the case of rat TRPM8-expressing HEK293 cells, antagonist/desensitizing behavior was evaluated against icilin at 0.25 µM and 0.10 µM. For icilin, efficacy was 75.1 ± 1.1 and potency EC_{50} = 0.11 ± 0.01 µM. In the case of HEK293 cells stably over-expressing recombinant rat TRPA1, the effects of TRPA1 agonists are expressed as a percentage of the effect obtained with 100 µM allyl isothiocyanate (AITC), which showed a potency of EC_{50} = 1.41 ± 0.04 µM and an efficacy of 65.9 ± 0.5.

The effect on $[Ca^{2+}]_i$ exerted by agonist alone was taken as 100%. Data are expressed as the concentration exerting a half-maximal inhibition of agonist-induced $[Ca^{2+}]_i$ elevation (IC_{50}), which was calculated again using GraphPad. All determinations were performed at least in triplicate. Statistical analysis of the data was performed by analysis of variance at each point using ANOVA followed by the Bonferroni's test.

Statistical methods

All statistical measures and methods are included in the respective Figure or Table captions. In brief: all data are shown as the mean ± SEM where applicable. A Student's *t*-test (unpaired, two-tailed) was used to determine differences between two groups. Data that included more than two groups or two factors were

analyzed by two-way ANOVA, with post-hoc Tukey HSD test. All statistical analyses were conducted using Excel or GraphPad Prism version 7, and a *p*-value less than 0.05 was considered significant throughout unless indicated otherwise. For the lipid profiling study (Figure 5.9), a Benjamini Hochberg correction (25 % false discovery rate) was applied.

A sample size of n=3 was sufficient to detect ≥ 50% inhibition of protein labeling with a 20% standard deviation and a power of 80% at a $p < 0.05$. Routinely, a protein is considered to be an off-target, if 50% inhibition of activity is reached at 10 µM. Since, BIA 10-2474 was weakly active on FAAH in in vitro assays (IC50 > 1 µM), the window of the ABPP assays was increased to a concentration of 50 µM detect off-targets.

Synthetic methods

General remarks

All reactions were performed using oven- or flame-dried glassware and dry solvents. Reagents were purchased from Sigma-Aldrich, Acros, and Merck and used without further purification unless noted otherwise. All moisture sensitive reactions were performed under an argon atmosphere.

^{1}H and ^{13}C NMR spectra were recorded on a Bruker AV 400 MHz spectrometer at 400.2 (^{1}H) and 100.6 (^{13}C) MHz using $CDCl_3$ as solvent, unless stated otherwise. Chemical shift values are reported in ppm with tetramethylsilane or solvent resonance as the internal standard ($CDCl_3$, δ 7.26 for ^{1}H, δ 77.16 for ^{13}C). Data are reported as follows: chemical shifts (δ), multiplicity (s = singlet, d = doublet, dd = double doublet, td = triple doublet, t = triplet, q = quartet, quintet = quint, br = broad, m = multiplet), coupling constants *J* (Hz), and integration. High-resolution mass spectra were recorded on a Thermo Scientific LTQ Orbitrap XL. Liquid chromatography was performed on a Finnigan Surveyor LC/MS system, equipped with a C18 column. Flash chromatography was performed using SiliCycle silica gel type SiliaFlash P60 (230–400 mesh). TLC analysis was performed on Merck silica gel 60/Kieselguhr F254, 0.25 mm. Compounds were visualized using $KMnO_4$ stain (K_2CO_3 (40 g), $KMnO_4$ (6 g), and water (600 mL)).

Synthesis of BIA 10-2639 (**6**) and BIA 10-2474 (**7**)

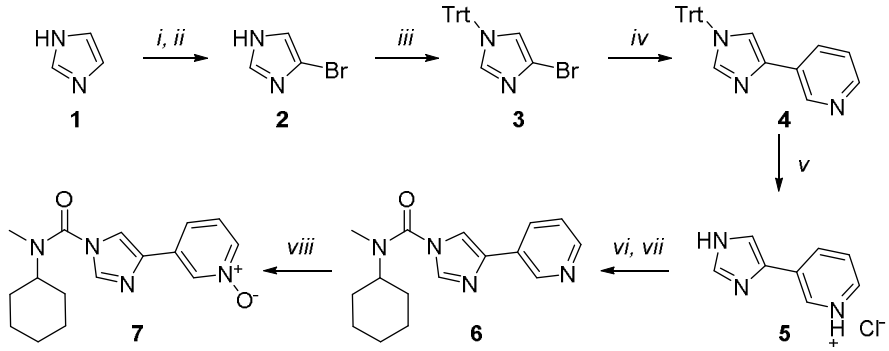

Scheme S5.1 | Reagents and conditions: *i)* NBS, DMF, RT; *ii)* 20% Na_2SO_3 (aq), 100 °C, 20%; *iii)* TrtCl, DIPEA, DMF, RT, 93%; *iv)* Cs_2CO_3, $Pd(PPh_3)_4$, pyridin-3-ylboronic acid, DMF:H_2O (8:1), 95 °C, 75%; *v)* 4N HCl in dioxane, MeOH, RT, 69%; *vi)* Na_2CO_3, triphosgene, *N*-methylcyclohexanamine, DCM, 0-20 °C; *vii)* cyclohexyl(methyl)carbamic chloride, 3-(1*H*-imidazol-4-yl)pyridine hydrochloride, DMAP, DIPEA, THF, reflux, 74%; *viii)* peracetic acid, DCM, 0-20 °C, 97%.

4-Bromo-1*H*-imidazole (**2**)

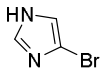

To a solution of 1*H*-imidazole **1** (4 g, 58.8 mmol) in DMF (100 mL) a solution of 1-bromopyrrolidine-2,5-dione (11.50 g, 64.6 mmol) in DMF (100 mL) was added over 1.5 h. Reaction left to stir for 110 h and concentrated to dryness. The residue obtained was taken up in 20% sodium sulfite solution in water and refluxed for 8 h. Upon cooling a precipitate formed which was filtered and dried to yield **2** (1.735 g, 11.81 mmol, 20%) as an off-white solid. ^{1}H NMR (400 MHz, MeOD) δ 7.61 (s, 1H), 7.11 (s, 1H). Spectroscopic data are in accordance with literature values.[39]

4-Bromo-1-trityl-1*H*-imidazole (**3**)

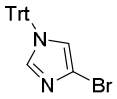

DIPEA (4.06 mL, 23.3 mmol) was added to a solution of trityl chloride (4.87 g, 17.5 mmol) and 4-bromo-1*H*-imidazole (1.71 g, 11.6 mmol) in DMF (20 mL). The resulting mixture was left to stir for 140 h. The resulting suspension was filtered and the yellowish solid was washed with methanol to yield a fine white solid which was purified by column chromatography to yield **3** (4.2 g, 11 mmol, 93%) as a white solid. ^{1}H NMR (400 MHz, $CDCl_3$) δ 7.43 – 7.30 (m, 10H), 7.19 – 7.04 (m, 6H), 6.80 (s, 1H). ^{13}C NMR (101 MHz, $CDCl_3$) δ 141.86, 138.71, 129.86, 128.45, 128.33, 120.90. Spectroscopic data are in accordance with literature values.[40]

3-(1-Trityl-1*H*-imidazol-4-yl)pyridine (**4**)

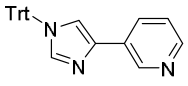

The title compound was synthesised under Suuzuki coupling conditions. Cesium carbonate (6.70 g, 20.6 mmol), **3** (2.00 g, 5.14 mmol) and pyridin-3-ylboronic acid (0.631 g, 5.14 mmol) were suspended in a mixture of DMF (40 mL) and water (5 mL). The resulting mixture was degassed by sonication for 30 min under a flow of argon. Tetrakis(triphenylphosphine)palladium(0) (148 mg, 0.128 mmol) was added and the mixture was heated to 90 °C for 16 h. The reaction mixture was diluted with EtOAc (100 mL) and washed with water. The organic layer was separated and the water layer extracted with EtOAc (2x 100 mL). The combined organic layers were washed with brine, dried ($MgSO_4$), filtered and concentrated. The oily residue was purified by column chromatography to yield **4** (1.50 g, 3.87 mmol, 75%) as a white solid. ^{1}H NMR (400 MHz, $CDCl_3$) δ 8.95 (m, 1H), 8.42 (m, 1H), 8.03 (m, 1H), 7.99 (s, 1H), 7.68 (m, 1H), 7.56 (d, *J* = 1.4 Hz, 1H), 7.47 – 7.40 (m, 1H), 7.34 (m, 9H), 7.24 (m, 1H), 7.24 – 7.16 (m, 7H). ^{13}C NMR (101 MHz, $CDCl_3$) δ 147.70, 146.42, 142.06, 139.66, 137.83, 132.04, 131.90, 129.97, 129.68, 128.15, 123.40, 117.92, 75.60.

3-(1*H*-Imidazol-4-yl)pyridine hydrochloride (**5**)

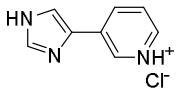

To a solution of **4** (1.24 g, 3.20 mmol) in MeOH HCl in dioxane (4 M, 4.0 mL) was added and the mixture was stirred for 1 h at RT. A white precipitate formed which was filtered off. The filtrate was vigorously stirred and pentane was slowly added to the mixture. More precipitate formed which was filtered off. The resulting solids were air dried to yield **5** (401.3 mg, 2.210 mmol, 69%). ^{1}H NMR (400 MHz, D_2O) δ 9.08 (d, *J* = 2.0 Hz, 1H), 8.84 (d, *J* = 1.3 Hz, 1H), 8.80 – 8.71 (m, 2H), 8.09 (dd, *J* = 8.3, 5.8 Hz, 1H), 8.00 (d, *J* = 1.3 Hz, 1H). ^{13}C NMR (101 MHz, D_2O) δ 143.10, 141.56, 138.96, 136.02, 127.80, 127.33, 127.14, 118.56.

N-Cyclohexyl-*N*-methyl-4-(pyridin-3-yl)-1*H*-imidazole-1-carboxamide (**6**)

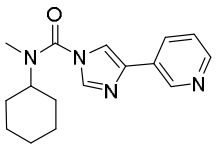

Triphosgene (0.831 g, 2.80 mmol) was added portionwise to a solution of *N*-methylcyclohexanamine (0.73 mL, 5.6 mmol) in DCM at 0 °C. After addition was complete, dried Na_2CO_3 (1.19 g, 11.2 mmol) was added in one batch and the mixture was allowed to warm to RT and stirred for 2 h. Na_2CO_3 was filtered off and the filtrate was concentrated to yield crude cyclohexyl(methyl)carbamic chloride which was used without further purification. To a stirred solution of **5** (203 mg, 1.12 mmol), DMAP (68.4 mg, 0.560 mmol) and DIPEA (0.587 mL, 3.36 mmol) in dry THF (40 mL) at 0 °C was added a solution of crude cyclohexyl(methyl)carbamic chloride in 5 mL THF. The resulting mixture was refluxed for 6 h under inert atmosphere. After the reaction was completed the cooled mixture was poured into saturated aqueous NH_4Cl solution and extracted three times with EtOAc. The combined organic layers were washed with brine, dried ($MgSO_4$), filtered and concentrated *in vacuo* to yield a white solid. Purification by column chromatography yielded an analytically pure sample of **6** (234 mg, 0.823 mmol, 74%). ^{1}H NMR (400 MHz, $CDCl_3$) δ 9.03 (dd, *J* = 2.3, 0.9 Hz, 1H), 8.54 (dd, *J* = 4.9, 1.6 Hz, 1H), 8.20 (dt, *J* = 8.0, 1.9 Hz, 1H), 7.94 (d, *J* = 1.3 Hz, 1H), 7.60 (d, *J* = 1.3 Hz, 1H), 7.41 (m, 1H), 3.95 (t, *J* = 12.0 Hz, 1H), 3.01 (s, 3H), 1.97 – 1.77 (m, 5H), 1.71 (d, *J* = 13.3 Hz, 1H), 1.59 (qd, *J* = 12.7, 12.2, 4.0 Hz, 2H), 1.46 – 1.31 (m, 2H), 1.14 (qt, *J* = 13.1, 3.5 Hz, 1H). ^{13}C NMR (101 MHz, $CDCl_3$) δ 150.98, 147.35, 145.67, 138.79, 137.47, 133.39, 129.63, 123.99, 114.32, 57.72, 31.42, 30.03, 25.44, 25.24. Spectroscopic data are in accordance with literature values.[41] HRMS (ESI+) m/z: calculated for $C_{16}H_{21}N_4O$ ([M+H]): 285.1710; found: 285.1710.

3-(1-(Cyclohexyl(methyl)carbamoyl)-1*H*-imidazol-4-yl)pyridine 1-oxide (**7**)

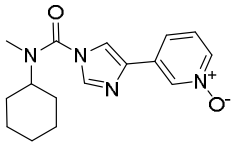

6 (100 mg, 0.352 mmol) was dissolved in dry DCM (25 mL) and cooled to 0 °C. Peracetic acid (0.119 mL, 0.703 mmol) as a 39% solution in acetic acid was added in one batch and the resulting mixture was stirred for 16 h. When TLC showed full conversion the reaction mixture was concentrated and purified by column chromatography to yield **7** (102.6 mg, 0.342 mmol, 97%) as a white solid. ^{1}H NMR (400 MHz, $CDCl_3$) δ 8.72 (t, *J* = 1.6 Hz, 1H), 8.18 (ddd, *J* = 6.4, 1.8, 1.0 Hz, 1H), 7.93 (d, *J* = 1.3 Hz, 1H), 7.77 (dt, *J* = 8.1, 1.2 Hz, 1H), 7.60 (d, *J* = 1.3 Hz, 1H), 7.34 (dd, *J* = 8.0, 6.4 Hz, 1H), 3.99 – 3.84 (m, 1H), 3.00 (s, 3H), 1.87 (t, *J* = 13.5 Hz, 4H), 1.71 (d, *J* = 13.4 Hz, 1H), 1.59 (qd, *J* = 12.8, 12.2, 3.9 Hz, 2H), 1.45 – 1.29 (m, 2H), 1.13 (qt, *J* = 13.1, 3.5 Hz, 1H). ^{13}C NMR (101 MHz, $CDCl_3$) δ 150.72, 137.84, 137.66, 136.75, 136.18, 133.22, 126.25, 124.17, 115.75, 57.95, 31.60, 30.13, 25.56, 25.33. Spectroscopic data are in accordance with literature values.[42] HRMS (ESI+) m/z: calculated for $C_{16}H_{21}N_4O_2$ ([M+H]): 301.1659; found: 301.1659.

Synthesis of three 2-step probes AJ167 (**8**), AJ179 (**9**) and AJ198 (**10**):

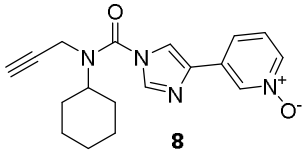

8

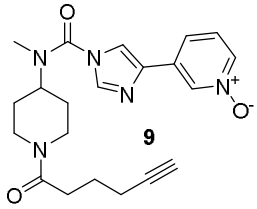

9

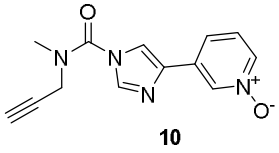

10

N-(Prop-2-yn-1-yl)cyclohexanamine (**11**)

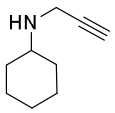

To a stirred solution of prop-2-yn-1-amine (0.50 mL, 7.8 mmol), cyclohexanone (0.404 mL, 3.90 mmol) and sodium triacetoxyborohydride (1.655 g, 7.81 mmol) in dry THF (40 mL) was slowly added one equivalent of acetic acid (0.223 mL, 3.90 mmol). The resulting mixture was stirred for 5 hours at room temperature after which the solvent was evaporated off. The crude was purified by column chromatography to yield **11** (0.521 g, 3.80 mmol, 97%) as a colourless oil. ^{1}H NMR (400 MHz, $CDCl_3$) δ 3.46 (d, *J* = 2.5 Hz, 2H), 2.74 – 2.59 (m, 1H), 2.21 (t, *J* = 2.4 Hz, 1H), 1.92 – 1.80 (m, 2H), 1.80 – 1.67 (m, 2H), 1.68 – 1.53 (m, 2H), 1.31 – 0.98 (m, 5H). ^{13}C NMR (101 MHz, $CDCl_3$) δ 82.51, 71.04, 54.95, 35.08, 33.01, 26.11, 24.83.

N-Cyclohexyl-*N*-(prop-2-yn-1-yl)-4-(pyridin-3-yl)-1*H*-imidazole-1-carboxamide (**12**)

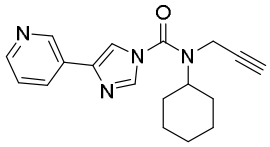

A solution of **11** (227 mg, 1.65 mmol) and triphosgene (163 mg, 0.551 mmol) in dry DCM (30 mL) was cooled to 0 °C and sodium carbonate (175 mg, 1.65 mmol) was added in one batch. The resulting suspension was stirred for 2 hours at room temperature. Na_2CO_3 was filtered off and the filtrate concentrated *in vacuo*. To a stirred solution of **5** (100 mg, 0.551 mmol), DMAP (67.3 mg, 0.551 mmol) and DIPEA (385 µL, 2.20 mmol) in dry THF (30 mL) at 0 °C was added a solution of crude carbamic chloride in 5 mL THF. The resulting mixture was refluxed for 4 hours under inert atmosphere. After the reaction was completed the cooled mixture was poured into saturated aqueous NH_4Cl solution and extracted three times with EtOAc. The combined organic layers were washed with brine, dried ($MgSO_4$), filtered and concentrated *in vacuo* to yield a white solid. This was purified by column chromatography to yield an analytically pure sample of **12** (110 mg, 0.357 mmol, 65%). ^{1}H NMR (500 MHz, $CDCl_3$) δ 9.02 (d, *J* = 2.2 Hz, 1H), 8.53 (dd, *J* = 1.6, 4.9 Hz, 1H), 8.17 (d, *J* = 1.3 Hz, 1H), 8.13 (dt, *J* = 1.9, 7.9 Hz, 1H), 7.82 (d, *J* = 1.3 Hz, 1H), 7.35 (dd, *J* = 4.8, 7.9 Hz, 1H), 4.09 (d, *J* = 2.4 Hz, 2H), 4.00 (tt, *J* = 3.7, 12.1 Hz, 1H), 2.49 (t, *J* = 2.4 Hz, 1H), 1.93 (ddt, *J* = 2.8, 13.7, 41.4 Hz, 4H), 1.70 (qd, *J* = 3.5, 12.4 Hz, 2H), 1.47 – 1.09 (m, 4H). ^{13}C NMR (126 MHz, $CDCl_3$) δ 150.70, 148.50, 146.69, 139.41, 132.62, 129.11, 123.74, 114.03, 79.91, 73.59, 58.82, 35.02, 30.55, 25.70, 25.26.

3-(1-(Cyclohexyl(prop-2-yn-1-yl)carbamoyl)-1*H*-imidazol-4-yl)pyridine 1-oxide AJ167 (**8**)

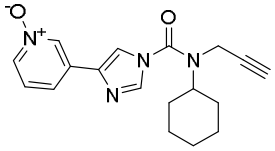

12 (20 mg, 0.065 mmol) is dissolved in dry DCM (10 mL) and cooled to 0 °C. Peracetic acid (20 µL, 0.118 mmol) as a 39% solution in acetic acid was added in one batch and the resulting mixture was stirred for 16 hours, slowly warming up to RT. The reaction mixture was concentrated and purified by column chromatography to yield **8** (11.5 mg, 0.035 mmol, 55%) as a white solid. ^{1}H NMR

(400 MHz, $CDCl_3$) δ 8.68 (s, 1H), 8.16 (d, *J* = 1.1 Hz, 2H), 7.86 – 7.80 (m, 1H), 7.75 (d, *J* = 8.0 Hz, 1H), 7.34 (t, *J* = 7.1 Hz, 1H), 4.07 (d, *J* = 2.4 Hz, 2H), 3.98 (tt, *J* = 12.0, 3.6 Hz, 1H), 2.49 (t, *J* = 2.4 Hz, 1H), 2.01 – 1.85 (m, 4H), 1.70 (qd, *J* = 12.2, 3.5 Hz, 2H), 1.46 – 1.10 (m, 4H). ^{13}C NMR (101 MHz, $CDCl_3$) δ 150.24, 137.87, 137.69, 137.04, 132.80, 126.02, 123.17, 115.26, 79.65, 73.80, 58.89, 35.01, 30.47, 25.64, 25.19. HRMS (ESI+) m/z: calculated for $C_{18}H_{20}N_4O_2$ ([M+H]): 325.1659; found: 325.1658.

1-(Hex-5-ynoyl)piperidin-4-one (**13**)

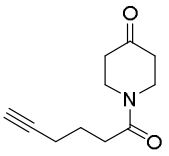

To a stirred solution of hex-5-ynoic acid (0.396 mL, 3.58 mmol) in a 1:1 mixture (v/v) of THF:DCM DIPEA (1.42 mL, 8.14 mmol) and HBTU (2.72 g, 7.16 mmol) were added in one batch. After the solution became homogenous piperidin-4-one hydrochloride hydrate (0.50 g, 3.3 mmol) was added. The mixture was left to stir for 215 h at room temperature. The reaction was quenched with saturated $NaHCO_3$ (aq.) and extracted three times with EtOAc. The combined organic layers were washed with brine, dried ($MgSO_4$), filtered and concentrated under reduced pressure. The residue was purified by column chromatography to yield **13** (572 mg, 2.96 mmol, 91%) as a colourless oil. ^1H NMR (400 MHz, $CDCl_3$) δ 3.90 (t, *J* = 6.4 Hz, 2H), 3.80 (t, *J* = 6.3 Hz, 2H), 2.58 (t, *J* = 7.3 Hz, 2H), 2.53 – 2.46 (m, 4H), 2.33 (td, *J* = 6.7, 2.7 Hz, 2H), 2.00 (t, *J* = 2.6 Hz, 1H), 1.91 (p, *J* = 7.0 Hz, 2H). ^{13}C NMR (101 MHz, $CDCl_3$) δ 206.91, 171.11, 83.64, 69.32, 44.06, 41.29, 40.90, 38.66, 31.43, 23.68, 17.92.

1-(4-(Methylamino)piperidin-1-yl)hex-5-yn-1-one (**14**)

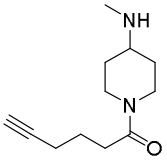

13 (572 mg, 2.96 mmol) was dissolved in DCM and methanamine hydrochloride (400 mg, 5.92 mmol), acetic acid (0.373 mL, 6.51 mmol) and DIPEA (1.09 mL, 6.22 mmol) were added. When cooled to 0 °C sodium triacetoxyborohydride (1.25 g, 5.92 mmol) was added in one portion. The resulting suspension was left to stir for 18 h warming up to RT. The reaction was quenched with a saturated aqueous Na_2CO_3 solution and extracted three times with EtOAc. The combined organic layers were washed with brine, dried ($MgSO_4$), filtered and concentrated *in vacuo*. The residue was purified by column chromatography to yield **14** (549 mg, 2.64 mmol, 89%) as a colorless oil. ^1H NMR (400 MHz, $CDCl_3$) δ 4.44 (m, 1H), 3.86 (m, 1H), 3.09 (m, 1H), 2.75 (m, 1H), 2.60 (m, 1H), 2.46 (t, *J* = 7.3 Hz, 2H), 2.44 (s, 3H), 2.27 (td, *J* = 6.8, 2.7 Hz, 2H), 2.01 (t, *J* = 2.6 Hz, 1H), 1.98 – 1.78 (m, 4H), 1.33 – 1.15 (m, 2H). ^{13}C NMR (101 MHz, $CDCl_3$) δ 170.30, 83.68, 69.02, 56.32, 43.98, 40.19, 33.42, 32.55, 31.72, 31.49, 23.84, 17.88.

N-(1-(Hex-5-ynoyl)piperidin-4-yl)-*N*-methyl-4-(pyridin-3-yl)-1*H*-imidazole-1-carboxamide (**15**)

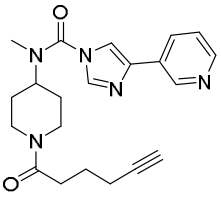

14 (274 mg, 1.32 mmol) was dissolved in DCM (25 mL) and cooled to 0 °C. Sodium carbonate (209 mg, 1.97 mmol) and triphosgene (390 mg, 1.32 mmol) were added and the mixture was stirred for 2 hours at RT. The solids were filtered off and the filtrate was concentrated under reduced pressure and redissolved in THF (25 mL). DIPEA (0.459 mL, 2.63 mmol), **5** (59.7 mg, 0.329 mmol) and DMAP (161 mg, 1.32 mmol) were added and the resulting mixture was refluxed for 4 h. The reaction was quenched with saturated aqueous $NaHCO_3$ solution and extracted three times with EtOAc. The organic layers were combined, washed with brine, dried ($MgSO_4$) and filtered. The solvent was removed and the crude purified by column chromatography to yield **15** (54.0 mg, 0.142 mmol, 43%) as a white solid. ^1H NMR (400 MHz, $CDCl_3$) δ 9.07 – 8.98 (m, 1H), 8.58 – 8.51 (m, 1H), 8.14 (m, 1H), 7.97 (d, *J* = 1.3 Hz, 1H), 7.61 (d, *J* = 1.3 Hz, 1H), 7.37 (dd, *J* = 7.9, 4.8 Hz, 1H), 4.85 (m, 1H), 4.29 (tt, *J* = 12.2, 4.2 Hz, 1H), 4.13 – 4.00 (m, 1H), 3.22 – 3.09 (m, 1H), 3.02 (s, 3H), 2.63 (m, 1H), 2.51 (t, *J* = 7.4 Hz, 2H), 2.31 (m, 2H), 1.99 (t, *J* = 2.6 Hz, 1H), 2.01 – 1.83 (m, 4H), 1.76 (qt, *J* = 12.2, 3.9 Hz, 2H). ^{13}C NMR (101 MHz, $CDCl_3$) δ 170.67, 151.29, 148.44, 146.52, 139.42, 137.50, 132.79, 129.05, 123.80, 114.03, 83.78, 69.20, 55.57, 44.62, 40.94, 32.15, 31.53, 29.23, 28.53, 23.80, 18.00.

3-(1-((1-(Hex-5-ynoyl)piperidin-4-yl)(methyl)carbamoyl)-1*H*-imidazol-4-yl)pyridine 1-oxide AJ179 (**9**)

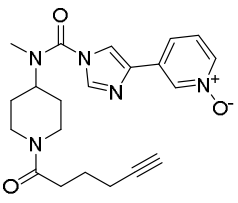

A solution of **15** (25 mg, 0.066 mmol) in DCM (25 mL) was cooled to 0 °C and peracetic acid (50 µL, 0.30 mmol) was added in one batch. The resulting mixture was left to stir for 16 h, after which the solvent was removed *in vacuo*. The resulting crude was purified by column chromatography to yield an analytically pure sample of **9** (4.5 mg, 0.011 mmol, 17%) as a white solid. ^1H NMR (400 MHz, MeOD) δ 8.82 (d, *J* = 1.7 Hz, 1H), 8.27 (d, *J* = 6.0 Hz, 1H), 8.22 (d, *J* = 1.2 Hz, 1H), 8.17 (d, *J* = 1.2 Hz, 1H),

8.05 (d, *J* = 8.3 Hz, 1H), 7.61 (dd, *J* = 8.1, 6.3 Hz, 1H), 4.73 (d, *J* = 13.3 Hz, 1H), 4.33 – 4.19 (m, 1H), 4.19 – 4.10 (m, 1H), 3.27 – 3.17 (m, 1H), 3.04 (s, 3H), 2.71 (dd, *J* = 14.0, 11.2 Hz, 1H), 2.61 – 2.55 (m, 2H), 2.32 – 2.25 (m, 2H), 2.06 (s, 1H), 2.02 – 1.74 (m, 6H). ^{13}C NMR (101 MHz, MeOD) δ 171.79, 151.05, 138.53, 137.24, 135.78, 135.46, 133.45, 126.77, 125.67, 116.99, 82.89, 68.90, 55.81, 44.57, 40.74, 31.16, 29.34, 28.56, 27.88, 24.03, 17.18.

N-Methyl-*N*-(prop-2-yn-1-yl)-4-(pyridin-3-yl)-1*H*-imidazole-1-carboxamide (**16**)

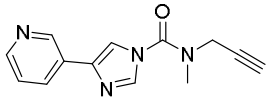

To a stirred solution of *N*-methylprop-2-yn-1-amine (0.084 ml, 1.0 mmol) in DCM (10 mL) at 0 °C sodium carbonate (106 mg, 1.00 mmol) was added. Triphosgene (223 mg, 0.750 mmol) was added and the mixture was stirred at RT for 1 hour. The suspension was then filtered and the filtrate was concentrated *in vacuo* to a yellow oil. This was redissolved in dry THF (10 mL, molecular sieves) and **5** (182 mg, 1.00 mmol) and DIPEA (0.437 mL, 2.50 mmol) were added. The mixture was heated and refluxed for 16 hours. The reaction was quenched by the addition of saturated aqueous $NaHCO_3$ and was extracted three times with EtOAc. The combined organic layers were washed with brine, dried ($MgSO_4$), filtered and concentrated. Purification using column chromatography yielded **16** (68 mg, 0.28 mmol, 28%). ^{1}H NMR (300 MHz, $CDCl_3$) δ 8.99 (s, 1H), 8.45 (d, *J* = 4.9 Hz, 1H), 8.30 – 8.13 (m, 2H), 8.02 (s, 1H), 7.47 (dd, *J* = 4.9, 8.1 Hz, 1H), 4.29 (d, *J* = 1.3 Hz, 1H), 3.22 (s, 4H), 2.93 (q, *J* = 2.1 Hz, 1H). ^{13}C NMR (75 MHz, $CDCl_3$) δ 148.78, 146.94, 134.57, 125.41, 116.53, 75.23, 40.81, 36.52, 30.74.

3-(1-(Methyl(prop-2-yn-1-yl)carbamoyl)-1*H*-imidazol-4-yl)pyridine 1-oxide AJ198 (**10**)

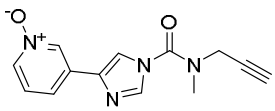

16 (20 mg, 0.083 mmol) was dissolved in DCM (10 mL) and cooled to 0 °C. Peracetic acid (92 µL, 0.42 mmol) as 30% solution in acetic acid was added in one batch. The mixture was stirred for 72 hours, slowly warming up to RT. The crude was concentrated under reduced pressure and purified by column chromatography to yield **10** (12 mg, 0.047 mmol, 56%) as a white solid. ^{1}H NMR (400 MHz, MeOD) δ 8.80 (t, *J* = 1.7 Hz, 1H), 8.25 (dt, *J* = 1.3, 6.5 Hz, 1H), 8.22 (d, *J* = 1.3 Hz, 1H), 8.15 (d, *J* = 1.3 Hz, 1H), 8.02 (dt, *J* = 1.2, 8.1 Hz, 1H), 7.58 (dd, *J* = 6.4, 8.1 Hz, 1H), 4.29 (d, *J* = 2.4 Hz, 2H), 3.22 (s, 3H), 2.92 (t, *J* = 2.5 Hz, 1H). HRMS (ESI+) m/z: calculated for $C_{13}H_{12}N_4O_2$ ([M+H]): 257.1033; found: 257.1037.

Supplementary Tables

Table S5.1 | Evaluating FAAH inhibitors against other endocannabinoid-related proteins. DAGL-α, DAGL-β, MAGL, ABHD6 and NAPE-PLD relative to DMSO as vehicle and [^{3}H]CP55940 displacement at overexpressing hCB1- and hCB2-receptor membranes.

Compound		hDAGL-α	mDAGL-β	hMAGL	hABHD6	hNAPE-PLD
		Remaining activity (%) ± SD				
BIA 10-2474	10 µM	102.7 ± 9.3	94.1 ± 4.3	117.9 ± 3.0	83.9 ± 8.2	96.9 ± 11.9
	30 µM	113.4 ± 4.0	102.9 ± 1.9	-	31.2 ± 13.2	-
	50 µM	-	-	-	-	95.9 ± 10.1
PF-04457845	10 µM	99.2 ± 8.7	105.5 ± 0.5	-	108.3 ± 21.6	98.6 ± 6.7
	30 µM	83.0 ± 8.4	106.2 ± 1.5	-	97.5 ± 26.7	-
	50 µM	-	-	-	-	70.2 ± 6.8
BIA 10-2639	10 µM	107.6 ± 2.6	94.5 ± 1.7	-	111.2 ± 8.3	89.0 ± 7.2
	30 µM	110.2 ± 3.2	102.1 ± 4.2	-	90.3 ± 11.2	-
	50 µM	-	-	-	-	89.9 ± 2.6

Table S5.1 (continued)

Compound		hCB$_1$	hCB$_2$
		Radioligand displacement (%) ± SEM	
BIA 10-2474	10 µM	29.8 ± 1.5	6.0 ± 5.4
	30 µM	-	-
	50 µM	38.4 ± 2.3	16.7 ± 8.9
PF-04457845	10 µM	59.9 ± 2.5	51.5 ± 4.6
	30 µM	-	-
	50 µM	103.8 ± 4.6	86.4 ± 1.3
BIA 10-2639	10 µM	36.8 ± 4.1	13.4 ± 8.0
	30 µM	-	-
	50 µM	44.0 ± 5.6	19.9 ± 5.4

Table S5.2 | Evaluating FAAH inhibitors for efficacy and affinity with TRPV-, TRPA1- and TRPM8-channels.

	TRPV1		TRPV2	
Compound	Efficacy (% ionomycin 4 µM)	IC_{50} (capsaicin 0.1 µM)	Efficacy (% ionomycin 4 µM)	IC_{50} (LPC 3 µM)
BIA 10-2474	< 10	> 20 µM	< 10	> 20 µM
PF-04457845	< 10	> 20 µM	< 10	> 20 µM
BIA 10-2639	< 10	> 20 µM	< 10	> 20 µM

	TRPV3		TRPV4	
Compound	Efficacy (% ionomycin 4 µM)	IC_{50} (thymol 100 µM)	Efficacy (% ionomycin 4 µM)	IC_{50} (GSK 10 nM)
BIA 10-2474	< 10	> 20 µM	< 10	> 20 µM
PF-04457845	< 10	> 20 µM	< 10	> 20 µM
BIA 10-2639	< 10	> 20 µM	< 10	> 20 µM

	TRPA1		TRPM8
Compound	Efficacy (%AITC 100 µM)	IC_{50} (AITC 100 µM)	IC_{50} (icilin 0.25 µM)
BIA 10-2474	< 10	> 20 µM	> 20 µM
PF-04457845	< 10	> 20 µM	> 20 µM
BIA 10-2639	< 10	> 20 µM	> 20 µM

References

1. Eddleston, M., Cohen, A. F. & Webb, D. J. Implications of the BIA-102474-101 study for review of first-into-human clinical trials. *Br. J. Clin. Pharmacol.* **81**, 582–586 (2016).
2. Butler, D. & Callaway, E. Scientists in the dark after French clinical trial proves fatal. *Nature* **529**, 263–264 (2016).
3. Kerbrat, A. *et al.* Acute Neurologic Disorder from an Inhibitor of Fatty Acid Amide Hydrolase. *N. Engl. J. Med.* **375**, 1717–1725 (2016).
4. Bégaud, B. *et al.* Report by the Temporary Specialist Scientific Committee (TSSC), 'FAAH (Fatty Acid Amide Hydrolase)', on the causes of the accident during a Phase 1 clinical trial. 1–28 (2016).
5. Cravatt, B. F. *et al.* Molecular characterization of an enzyme that degrades neuromodulatory fatty-acid amides. *Nature* **384**, 83–87 (1996).
6. Kathuria, S. *et al.* Modulation of anxiety through blockade of anandamide hydrolysis. *Nat. Med.* **9**, 76–81 (2002).
7. Devane, W. A. *et al.* Isolation and structure of a brain constituent that binds to the cannabinoid receptor. *Science* **258**, 1946–1949 (1992).
8. Long, J. Z. *et al.* Dual blockade of FAAH and MAGL identifies behavioral processes regulated by endocannabinoid crosstalk in vivo. *Proc. Natl. Acad. Sci.* **106**, 20270–20275 (2009).
9. van der Stelt, M. *et al.* Anandamide acts as an intracellular messenger amplifying Ca2+ influx via TRPV1 channels. *EMBO J.* **24**, 3026–3037 (2005).
10. Hampson, A. J. *et al.* Dual effects of anandamide on NMDA receptor-mediated responses and neurotransmission. *J. Neurochem.* **70**, 671–676 (1998).
11. Huggins, J. P., Smart, T. S., Langman, S., Taylor, L. & Young, T. An efficient randomised, placebo-controlled clinical trial with the irreversible fatty acid amide hydrolase-1 inhibitor PF-04457845, which modulates endocannabinoids but fails to induce effective analgesia in patients with pain due to osteoarthritis of th. *Pain* **153**, 1837–1846 (2012).
12. Li, G. L. *et al.* Assessment of the pharmacology and tolerability of PF-04457845, an irreversible inhibitor of fatty acid amide hydrolase-1, in healthy subjects. *Br. J. Clin. Pharmacol.* **73**, 706–716 (2012).
13. Niphakis, M. J. & Cravatt, B. F. Enzyme Inhibitor Discovery by Activity-Based Protein Profiling. *Annu. Rev. Biochem.* **83**, 341–377 (2014).
14. Baggelaar, M. P. *et al.* Development of an Activity-Based Probe and In Silico Design Reveal Highly Selective Inhibitors for Diacylglycerol Lipase-α in Brain. *Angew. Chemie Int. Ed.* **52**, 12081–12085 (2013).
15. Liu, Y., Patricelli, M. P. & Cravatt, B. F. Activity-based protein profiling: The serine hydrolases. *Proc. Natl. Acad. Sci.* **96**, 14694–14699 (1999).
16. Ogasawara, D. *et al.* Rapid and profound rewiring of brain lipid signaling networks by acute diacylglycerol lipase inhibition. *Proc. Natl. Acad. Sci.* **113**, 26–33 (2016).
17. Baggelaar, M. P. *et al.* Highly Selective, Reversible Inhibitor Identified by Comparative Chemoproteomics Modulates Diacylglycerol Lipase Activity in Neurons. *J. Am. Chem. Soc.* **137**, 8851–8857 (2015).
18. Ahn, K. *et al.* Mechanistic and Pharmacological Characterization of PF-04457845: A Highly Potent and Selective Fatty Acid Amide Hydrolase Inhibitor That Reduces Inflammatory and Noninflammatory Pain. *J. Pharmacol. Exp. Ther.* **338**, 114–124 (2011).
19. Maccarrone, M. *et al.* Anandamide Hydrolysis by Human Cells in Culture and Brain. *J. Biol. Chem.* **273**, 32332–32339 (1998).
20. Johnson, D. S. *et al.* Discovery of PF-04457845: A Highly Potent, Orally Bioavailable, and Selective Urea FAAH Inhibitor. *ACS Med. Chem. Lett.* **2**, 91–96 (2011).
21. Rostovtsev, V. V., Green, L. G., Fokin, V. V. & Sharpless, K. B. A Stepwise Huisgen Cycloaddition Process: Copper(I)-Catalyzed Regioselective "Ligation" of Azides and Terminal Alkynes. *Angew. Chemie Int. Ed.* **41**, 2596–2599 (2002).
22. van Esbroeck, A. C. M. *et al.* Activity-based protein profiling reveals off-target proteins of the FAAH inhibitor BIA 10-2474. *Science* **356**, 1084–1087 (2017).
23. Thomas, G. *et al.* The Serine Hydrolase ABHD6 Is a Critical Regulator of the Metabolic Syndrome. *Cell Rep.* **5**, 508–520 (2013).
24. Chang, P.-A. & Wu, Y.-J. Neuropathy target esterase: An essential enzyme for neural development and axonal maintenance. *Int. J. Biochem. Cell Biol.* **42**, 573–575 (2010).
25. Shayman, J. A. & Abe, A. Drug induced phospholipidosis: an acquired lysosomal storage disorder. *Biochim. Biophys. Acta* **1831**, 602–11 (2013).
26. Ross, M. K., Streit, T. M. & Herring, K. L. Carboxylesterases: Dual roles in lipid and pesticide metabolism. *J. Pestic. Sci.* **35**, 257–264 (2010).
27. Wei, B. Q., Mikkelsen, T. S., McKinney, M. K., Lander, E. S. & Cravatt, B. F. A second fatty acid amide hydrolase with variable distribution among placental mammals. *J. Biol. Chem.* **281**, 36569–78 (2006).
28. Li, Y. *et al.* Carboxylesterase 2 prevents liver steatosis by modulating lipolysis, endoplasmic reticulum stress, and lipogenesis and is regulated by hepatocyte nuclear factor 4 alpha in mice. *Hepatology* **63**, 1860–1874 (2016).

29. Richardson, R. J., Hein, N. D., Wijeyesakere, S. J., Fink, J. K. & Makhaeva, G. F. Neuropathy target esterase (NTE): overview and future. *Chem. Biol. Interact.* **203**, 238–44 (2013).
30. Read, D. J., Li, Y., Chao, M. V, Cavanagh, J. B. & Glynn, P. Neuropathy target esterase is required for adult vertebrate axon maintenance. *J. Neurosci.* **29**, 11594–600 (2009).
31. Moser, M. *et al.* Cloning and expression of the murine sws/NTE gene. *Mech. Dev.* **90**, 279–82 (2000).
32. Bertrand, D., Bertrand, S., Neveu, E. & Fernandes, P. Molecular characterization of off-target activities of telithromycin: a potential role for nicotinic acetylcholine receptors. *Antimicrob. Agents Chemother.* **54**, 5399–402 (2010).
33. Bachovchin, D. A. *et al.* Superfamily-wide portrait of serine hydrolase inhibition achieved by library-versus-library screening. *Proc. Natl. Acad. Sci.* **107**, 20941–20946 (2010).
34. Hu, C. *et al.* RPLC-ion-trap-FTMS method for lipid profiling of plasma: method validation and application to p53 mutant mouse model. *J. Proteome Res.* **7**, 4982–91 (2008).
35. Gattinoni, S. *et al.* Enol carbamates as inhibitors of fatty acid amide hydrolase (FAAH) endowed with high selectivity for FAAH over the other targets of the endocannabinoid system. *ChemMedChem* **5**, 357–360 (2010).
36. van der Wel, T. *et al.* A natural substrate-based fluorescence assay for inhibitor screening on diacylglycerol lipase α. *J. Lipid Res.* **56**, 927–935 (2015).
37. Peppard, J. V, Mehdi, S., Li, Z. & Duguid, M. S. Assay methods for identifying agents that modify the activity of NAPE-PLD or ABHD4 (WO2008150832A1). (2008).
38. Mukhopadhyay, P. *et al.* The novel, orally available and peripherally restricted selective cannabinoid CB 2 receptor agonist LEI-101 prevents cisplatin-induced nephrotoxicity. *Br. J. Pharmacol.* **173**, 446–458 (2016).
39. Sandtorv, A. H. & Bjørsvik, H.-R. Fast Halogenation of Some N - Heterocycles by Means of N , N′ -Dihalo-5,5-dimethylhydantoin. *Adv. Synth. Catal.* **355**, 499–507 (2013).
40. Roumen, L. *et al.* Synthesis, Biological Evaluation, and Molecular Modeling of 1-Benzyl-1 H -imidazoles as Selective Inhibitors of Aldosterone Synthase (CYP11B2). *J. Med. Chem.* **53**, 1712–1725 (2010).
41. Bial - Portela and Ca, S. A., Russo, D., Wahnon, J. B. R., Maton, W. & Eszenyi, T. Process for the synthesis of substituted urea compounds (WO2014017938A2). (2014).
42. Kiss, L. E. *et al.* Pharmaceutical Compounds (WO2010074588A2). (2010).